A novel nanoemulsion based microalgal growth medium for enhanced biomass production

Harshita Nigam
Indian Institute of Technology Delhi
Anushree Malik
Indian Institute of Technology Delhi https://orcid.org/0000-0002-2761-0568
Vikram Singh (vs225@chemical.iitd.ac.in)
Indian Institute of Technology Delhi

Research

Keywords: Microalgae, Nanoemulsion, Paraffin oil, Silicone oil, Biomass

Posted Date: December 28th, 2020

DOI: https://doi.org/10.21203/rs.3.rs-43578/v2

Version of Record: A version of this preprint was published at Biotechnology for Biofuels on April 30th, 2021. See the published version at https://doi.org/10.1186/s13068-021-01960-8.

Title: A novel nanoemulsion based microalgal growth medium for enhanced biomass production

Harshita Nigam[1], Anushree Malik[1*], Vikram Singh[2*]

[1]Applied Microbiology Laboratory, Centre for Rural Development and Technology and [2]Complex Fluid Lab, Department of Chemical Engineering, Indian Institute of Technology Delhi, New Delhi, Hauz Khas, New Delhi 110016, India

Email address:

harshitanigam31@gmail.com (H. Nigam)

anushree@rdat.iitd.ac.in (A. Malik)

vs225@chemical.iitd.ac.in (Vikram Singh)

Corresponding author:

1. Assistant Prof.Vikram Singh*

Address: Room No- 377, Block II

Department of Chemical Engineering, Indian Institute of Technology Delhi, Hauz Khas, New Delhi 110016, India

Phone: +91 8586809653, +91 11 2659 1030

Email: vs225@chemical.iitd.ac.in,

Prof. Anushree Malik*

Address: Room No- 271, Block III

Centre for Rural Development and Technology, Indian Institute of Technology Delhi,

Hauz Khas, New Delhi 110016, India

Phone: +91 9968294221

Email: anushree@rdat.iitd.ac.in

Graphical Abstract:

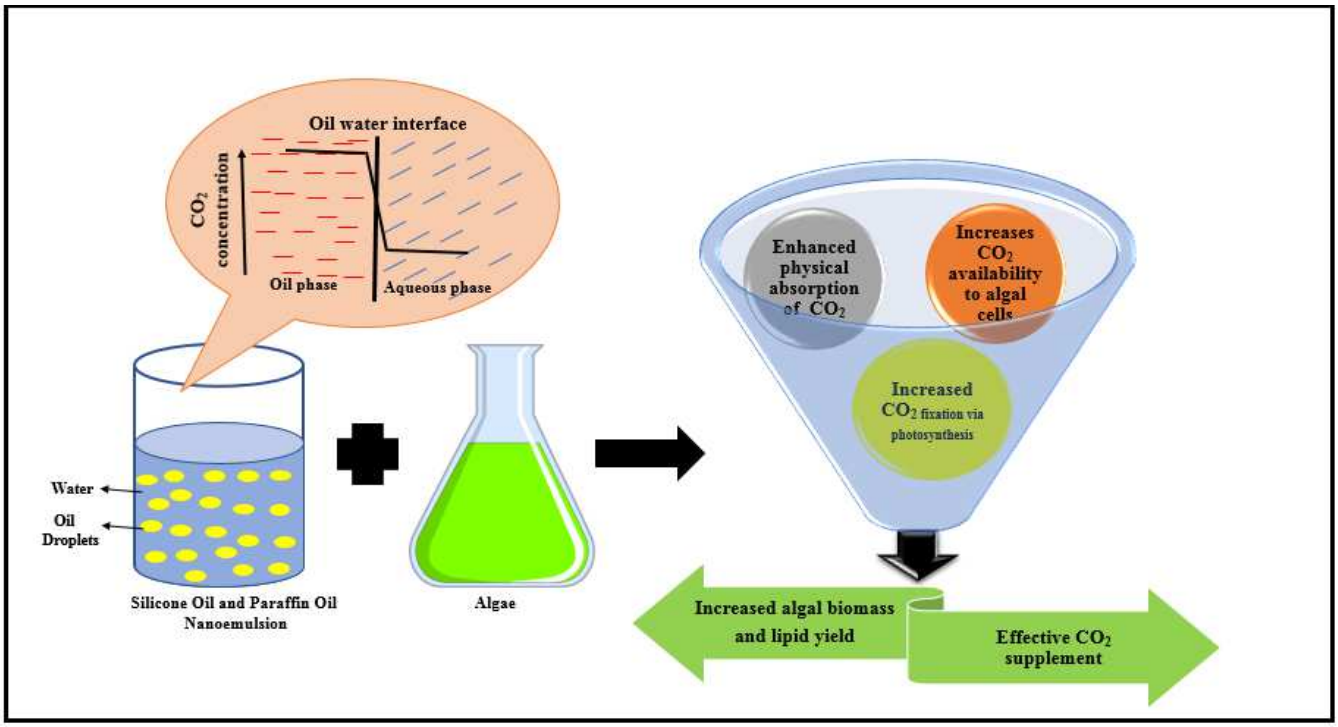

Abstract

Background: Microalgae are well-established feedstocks for applications ranging from biofuels to valuable pigments and therapeutic proteins. However, the low biomass productivity using commercially available growth mediums is a roadblock for its mass production. This work describes a strategy to boost the algal biomass productivity by using an effective CO_2 supplement.

Results: In the present study, a novel nanoemulsion-based media has been tested for the growth of freshwater microalgae strain Chlorella pyrenoidosa. Two different nanoemulsion-based media were developed using 1% silicone oil nanoemulsion (1% SE) and 1% paraffin oil nanoemulsion (1% PE) supplemented in BG11 media During 12-day growth experiment, the 1% PE gave the highest biomass yield (3.2± 0.07gL^{-1}), followed by 1%SE (2.75 ± 0.07 gL^{-1}) and control (1.03±0.02 gL^{-1}). The respective microalgal cell number measured using cell counter were (3.0 ± 0.21 x 10^6 cells ml^{-1}), (2.4 ± 0.30 x 10^6 cells ml^{-1}) and (1.34 ± 0.09 x 10^6 cells ml^{-1}). Cell viability analysis using MTT assay showed that 1% PE also had higher viable cells (94%) compared to 1% SE (77%) and control (53%). The effective CO_2 absorption tendency of the emulsion was highlighted as the key mechanism for greater biomass production. On the biochemical characterization of the produced biomass, it was found that the nanoemulsion cultivated *C. pyrenoidosa* had increased lipid (1% PE=26.8%, 1% SE=23.6%) and carbohydrates (1% PE=17.2%, 1% SE=18.9%) content compared to the control (lipid=18.05%, carbohydrates=13.6%).

Conclusions: This study provides a novel nanoemulsion which acts as an effective CO_2 supplement for microalgal growth media which increase the growth of microalgal cells. Importantly, nanoemulsions cultivated microalgal biomass possess increment in lipid and carbohydrate content. This approach also provides high microalgal biomass productivity without alteration of morphological characteristics like cell shape and cell size.

Keywords: Microalgae, Nanoemulsion, Paraffin oil, Silicone oil, Biomass

1. Background:

One of the major challenges in algal cultivation is the limited supply of CO_2 from the atmosphere to the cultivation system due to poor CO_2 transfer rate from air to water (1). Finding suggests that the diffusion of CO_2 from the atmosphere to water cannot meet the photosynthetic efficiency of algae (2). In this regard, most of the research has been focused on the delivery of CO_2 to photobioreactors, raceways, and ponds directly using air pumps, but this approach has two main limitations. Firstly, the delivery of CO_2 in such a manner is an energy-intensive process (3), and secondly, most of the CO_2 escape in the surroundings leading to its loss. To overcome these limitations, chemical absorption of the carbon dioxide has been considered in the past, which involves the addition of solvents like carbonates (4), amines (5), and piperazine (6). However, these processes are energy-intensive and possess economic and technical limitations (7). In a recent finding, solvent-based CO_2 delivery was proposed which involves the capture of CO_2 in the solvent and its subsequent delivery to algal cells through the non-porous membrane e.g. Polydimethylsiloxane (PDMS) membrane (8). This membrane-based system allows diffusion of CO_2 from solvent into algal cultivation media. However, with this approach, the cost of membrane adds significant capital burden for large scale systems (9).

Therefore, an efficient CO_2 delivery agent to the algal cultivation media is required which can be used to increase the growth, productivity, and synthesis of biomolecules inside algal cells. Moreover, the CO_2 delivery agent should be cost-effective, non-toxic, and should have a high affinity for CO_2. Thus, the present study seeks to explore the two inert organic solvents named silicone oil and paraffin oil in the form of oil-in-water nanoemulsion for the cultivation of algae.

These inert organic solvents absorb CO_2 through physical absorption without having any chemical reaction. The binding responsible for physical absorption is being either Van der Waals type or electrostatic between the CO_2 and solvent molecules (10). The driving force responsible for physical absorption is the high solubility of CO_2 in the solvent.

To improve the physical absorption process, the concept of using nanoemulsion to capture CO_2 has been proposed. Research literature suggests that the inert organic solvents like perfluorodecalin (11), are effective in delivering CO_2 to algal cells. However, their formulation in the form of nanoemulsion for the algal cultivation area is unexplored. The physiochemical properties like nano-size, stability against gravitational separation, easy handling (12) and, the use of ingredients, which govern the functionality of the nanoemulsions, make it a suitable choice for the absorption of CO_2.

Hence, the present study focused on formulating oil-in-water nanoemulsion and its integration to *Chlorella pyrenoidosa* cultivation (13). The aim was to develop an effective growth supplement and study its effect on algal cell growth, morphology, pigment synthesis, biomass productivity, and biomass composition. In the end, other possible mechanisms have been highlighted that could have devoted to greater algal biomass production due to prepared nanoemulsions.

2. MATERIALS AND METHODS:

2.1. Selection of oil and surfactant:

Silicone, paraffin oil, and surfactant (Tween 80) were procured from Central Drug House (New Delhi, India). Silicone oil is a nonpolar solute, having a kinematic viscosity of 300cS and has efficient gaseous absorption capacity which makes it suitable oil for our experiment. Paraffin oil

is a mixture of C_{10}–C_{15} alkanes and cycloalkanes which are colorless, antioxidative, and have low viscosity.

The nonionic surfactant Tween 80 (Polyoxyethylene (20) sorbitan monooleate) with HLB of 18, was used for the formulation of silicone and paraffin oil nanoemulsion. The surfactant action is to reduce the interfacial tension (IFT) between two phases (14).

2.2. Formulation of Nanoemulsion

The silicone and paraffin oil-in-water nanoemulsions were prepared by a high energy method (13). Nanoemulsion was formulated by adding an aqueous phase in a mixture of oil and surfactant. The resulting mixture was homogenized at 10,000rpm for ~15 minutes at 25 ºC (OV5, VELP Scientifica, Italy) and the nanoemulsion was subjected to ultrasonic emulsification by using 20 kHz EI-1000UP ultrasonicator (Electrosonic Industries, India) using 15mm titanium probe; the sonicator having sequential cycles of 45 min, with sequential on and off.

2.3. Characterization and stability analysis of silicone and paraffin oil nanoemulsion (Gravimetric method and Droplet size observation by Dynamic Light Scattering)

The resultant nanoemulsion was visually observed, to analyze the change in physical appearance. Nearly 25 ml of silicone and paraffin oil nanoemulsion kept undisturbed in an 80 ml beaker at 25ºC were observed for sedimentation or creaming for 15 days. The average diameter of the droplet size of silicone and paraffin oil nanoemulsion was observed by Dynamic Light Scattering (DLS) by photon associated spectrometer Malvern 4700 zeta-sizer (Anton Paar, Austria) equipped with an argon laser at a wavelength of 488nm. The temperature of the nanoemulsions was maintained at 25ºC and the scattering angle was fixed at 90º. The samples

were withdrawn at the 0^{th} day and 15^{th} day and observed for DLS study. The determination of the droplet size of silicone oil and paraffin oil nanoemulsions was carried out by diluting 1ml of the sample with 10 ml of water to avoid multiple scattering.

2.4. Dissolved CO_2 analysis by titrimetric method

The dissolved CO_2 concentration (DCC) in the sample was determined by APHA (15). The sample was titrated with NaOH solution (0.01 N) using phenolphthalein as an indicator. The colorless phenolphthalein indicator was used to recognize the endpoint of the reaction. All titrations were performed at room temperature and proper stirred condition and volume of NaOH was recorded. The dissolved CO_2 concentration was determined by the mentioned formula.

$$CO_2\,(mgL^{-1}) = \frac{[\text{Volume of NaOH} \times \text{Conc. of NaOH (in Normality)} \times 22 \times 1000]}{\text{Volume of the sample}} \quad (1)$$

2.5. Selection of algal strain and inoculum development:

Pure culture of micro-algal species *Chlorella pyrenoidosa* was previously procured from the National Collection of Industrial Microorganisms (NCIM), NCL Pune (India). BG 11 broth of HiMedia M1541 was used as standard algal growth media. The algal culture was maintained in the algal growth chamber under LED light source ~ 46.5 to 50 µmol $m^{-2}s^{-1}$ to provide the required photon flux density for photosynthesis of microalgal cultures with light and dark cycle of 12: 12 hours. The incubation temperature of microalgal cultivation was 25± 1 ºC.

The inoculum of pure micro-algal strain *C. pyrenoidosa* was cultured in BG11 media using 250 mL Erlenmeyer flasks in controlled conditions (16). During the log phase of the growth cycle,

30% of microalgal cell culture was used as inoculum for experimental units with an initial absorbance of 2.0 at 680 nm.

2.6. Experimental set -up

The experiments were conducted in controlled conditions. The developed 100ml of silicone oil and paraffin oil nanoemulsion was mixed with 0.16 g BG11 growth media and inoculated with *C. pyrenoidosa.* The control was used for the respective set of experiments (*C. pyrenoidosa* in BG11 without silicone and paraffin oil nanoemulsion). The time duration of experiments was 12 days and performed in duplicates. The experimental flasks were incubated in continuous shaking mode (~150 rpm) at temperature 25± 1 ℃ and light intensity ~ 46.5 to 50 µmol $m^{-2}s^{-1}$ respectively.

The growth of *C. pyrenoidosa* was observed by measuring optical density at 680nm, chlorophyll-a estimation and pH change at a regular interval of 48 hours. Additionally, the viability testing of micro-algal cells was performed via MTT and SYTOX green staining on the 8^{th} day of the experiment. Further, the harvested microalgal biomass was characterized by FESEM and FTIR after the 12^{th} day.

2.7. Analytical Techniques

Micro-algal growth in formulated nanoemulsion

The optical density of *C. pyrenoidosa* was measured at 680 nm by using U.V-Vis spectrophotometer (Lambda 35, Perkin Elmer, USA). The aliquots of the 2-ml algal sample were withdrawn from well-mixed microalgal culture from the experimental unit and centrifuged at

3600 g for 5 minutes. The obtained pellets were washed three- four times by PBS buffer and surfactant (Tween 80) to remove silicone and paraffin oil nanoemulsions. The resultant pellets were resuspended in 2-ml distilled water and placed in the cuvette for observation.

The pH of microalgal cells cultivated in nanoemulsions was measured by pH meter (10BN, Eutech, U.S) at a regular interval of 48 hours. Chlorophyll-a estimation was performed by the method prescribed by Chinnasamy *et al*., 2010 (17). The 2 ml of microalgal cell suspension was collected in microcentrifuge tubes and centrifuged at 3600g for 10 min. The pellet formed was resuspended in 2 ml of methanol after decanting and placed in the water bath for chlorophyll extraction at 60ºC for ~30 minutes. The chlorophyll content in the supernatant was observed spectrophotometrically at 750, 665.2 and 652 nm, and then calculated by Porra's equation (18):

$$C\text{hl a } (\mu g\ ml^{-1}) = 16.29\ (A^{665.2}-A^{750}) - 8.54\ (A^{652}-A^{750}) \qquad (2)$$

where, A^{750}, $A^{665.2,}$ and A^{652} are the absorbance of the chlorophyll in methanol, respectively.

Samples of experiments were subjected to the determination of biomass growth (dry cell weight) on the 13th day. The 50 ml samples were centrifuged (R-8C, REMI, INDIA) at 3600 g for 10 min then decant the supernatant. The pellets were washed as mentioned previously. The remaining pellets were suspended in distilled water (volume made upto 50 ml) and filtered with pre-weighed Whatman filters. The filters with microalgal biomass were subjected to oven-dry at 60ºC for 24 hours and then cooled at room temperature in a desiccator and weighed (19). Dried microalgal biomass was determined gravimetrically to evaluate the dry cell weight (gL^{-1}) (20). Additionally, cell counting was performed by using cellometer (Catalog No. CHT4-PD100,

142 Nexcelom Bioscience LLC). The data was noted, and averages of the duplicates were plotted in
143 the graph with standard deviation as error bar.

144 **2.8. Biochemical composition:**

145 After harvesting, the microalgal biomass was dried at 65-70ºC for 48 hr for biochemical
146 compositional analysis (till a constant mass is reached). Phenol-sulfuric acid was used for the
147 analysis of total carbohydrate content (21). Dried algal biomass (50mg) was hydrolyzed with
148 2.5N HCl (2.5ml) and placed in a water bath for 3 hours at 100ºC, followed by cooling at room
149 temperature and neutralized with sodium carbonate. After neutralization, 0.1ml sample was
150 pipette out in a fresh tube and diluted to 1 ml. After dilution, 1ml phenol and 5ml sulfuric acid
151 were mixed and cooled in the water bath at 25-30ºC. The absorbance of the sample was
152 measured at 490nm and the total carbohydrate was calculated using the standard calibration
153 curve of glucose. Alkaline hydrolysis was performed, and total protein content was measured by
154 Folin-Lowery method (22).

155 Total lipid content was determined by modified Bligh and Dryer's method (23). The microalgal
156 cell wall was ruptured by heat treatment at 100-110ºC up to 5 minutes for efficient extraction.
157 The chloroform-methanol mixture (1:1 v/v) was added to the sample in the proportion of 1:1 and
158 lipid was estimated gravimetrically.

159 **2.9. Viability testing of microalgal cells cultivated in silicone oil nanoemulsion and**
160 **microscopic analysis:**

161 To determine the viability of microalgal cells, 3-[4,5-dimethylthiazol-2-yl]-2,5-
162 diphenyltetrazoliumbromide (MTT) was performed. The 5 mg ml^{-1} of MTT dye was formed by
163 dissolving in Phosphate Saline Buffer (PBS). The PBS washed the microalgal pellets of 2ml
164 culture, followed by the addition of MTT dye (final concentration 0.5 mg ml^{-1}) and incubate at
165 37ºC for 4 hours. After removal of MTT dye solution from microalgal cells, DMSO and
166 isopropanol (1:1) were added. The result was observed by taking absorbance at 570 nm and data
167 were expressed in the form of relative viability in percentage (24).

168 $$Relative\ viability\ = (Absorbance\ of\ treated\ cells \div Absorbance\ of\ control)\ \times 100 \quad (3)$$

169 Additionally, the viable cells were assessed by exposing the samples to nucleic acid stain
170 SYTOX green (Cat. No. S7020, Invitrogen). The Sytox stock solution of 50 µM was prepared
171 and 5 µL of stock solution was added to 95 µL microalgal samples, resulting in a final dye
172 concentration of 5 µM (25). Samples were incubated at room temperature in the dark for 30
173 min. The stained samples were loaded on a slide and placed into a fluorescence microscope
174 (Nikon Eclipse Ti-2 inverted microscope). The fluorescence of stained cells was observed at
175 100X magnification and images were captured using digital camera connected to the
176 microscope.

177 **2.10. Spectroscopic analysis by FTIR:**

178 The known volume of suspension was withdrawn and centrifuged at 3600g for 10 minutes. The
179 pellets were washed 2-3 times with phosphate saline buffer (PBS) of 0.15M and placed for
180 lyophilization (Allied Frost FD3). The dried microalgal powder was ground and homogenized with

KBr at the ratio of 1:100, and the mixture was pressed by a molding machine with a pressure load of 200 kg cm^{-2} for 5 minutes. The fine KBr pellet was prepared and placed at Deuterated triglycine sulfate (DTGS) detector of Nicolet Is50 (Thermo Scientific) FT-IR spectrometer (26). The transmittance spectra were collected between 400 cm^{-1} to 4000 cm^{-1} with 64 scans.

2.11. Microscopic analysis:

Surface morphology and cell size were detected by Field Emission Scanning Electron Microscopy (FESEM, JSM-7800F Prime, Jeol). The microalgal suspension was centrifuged at 3600g for 5- 10 minutes. The resultant pellet was washed 2-3 times with 0.15 M phosphate saline buffer (pH 6.8). After washing, the pellet was fixed using the fixative solution (2.5% glutaraldehyde) for 30 minutes. The resultant pellets were washed in phosphate saline buffer 3-4 times followed by serially dehydrated with 25%, 50%, 75%, 90%, and 100% ethanol, respectively. Finally, the fixed cells were dried at room temperature and coated with Platinum (27).

2.12. Statistical Analysis:

All the experiments were performed in duplicates. The results presented here are mean of the duplicates, mean ± standard deviation, or mean with error bars in graphs unless mentioned otherwise.

3. RESULTS AND DISCUSSION:

3.1. Nanoemulsion Stability Analysis:

The stability of nanoemulsion was observed in terms of their appearance and droplet size (28). The samples were stored undisturbed for 15 days at 25 ºC for observation. On visual observation, there was no creaming and flocculation in the nanoemulsion during the storage period. Additionally, the stability of the nanoemulsions was evaluated by droplet size measurement. A rapid increase in droplet size corresponds to that the stability of the nanoemulsion is low. Figure. 1 displays the droplet size of 1% SE and 1% PE on the 0^{th} day and 15^{th} day, respectively. The average droplet size observed in 1% SE was in the range of ~ 244 nm to 285 nm and ~ 164 nm to 297nm in 1% PE. As evident from Figure. 1, the size of the maximum droplets of nanoemulsions were stable over a period of 15 days. The result indicated that the larger droplet size, greater than a micron have been separated from the emulsion.

3.3. Growth of Microalgae in Nanoemulsions:

In the present study, 1% SE and 1% PE were prepared to test its potential in microalgal cultivation. The microalgal cell growth in formulated nanoemulsions were evaluated by the following parameters: optical density at 680 nm, pH, chl-a, biomass yield, and cell count.

Interestingly, for both the nanoemulsions, *C. pyrenoidosa* showed an increase in growth compared with conventional BG11 media (control). Results obtained from measuring OD_{680}, showed that ~ 1.6 folds growth was observed in1% SE supplemented growth medium compared with control on the 10^{th} day. On the other hand, 1% PE growth medium gave an increment of ~ 1.8 folds in microalgal cell growth compared with control. In 1% SE and 1% PE supplemented microalgal cultivation systems, the rapid exponential growth phase was observed from day-1

compared with control. This exponential growth lasted till the 10^{th} day of the microalgal cultivation in nanoemulsions while in control it lasted till the 8^{th} day.

Gonçalves et al., 2016 reported that the increased CO_2 concentration in the microalgal cultivation system prolonged the exponential phase (31). Araujo et al., 2005 observed via cultivating diatom (*Chaetoceros cf. wighamii*) that the addition of carbon dioxide prolonged the exponential phase and this phase of the life span of microalgae own highest nutritional value which can be used as feed for aquatic animals (32,33). In the proposed study, the growth pattern including the duration of exponential phases was quite similar for both the nanoemulsions. The microalgal cell growth during the exponential phase was much higher in nanoemulsion systems compared with control (Figure. 2).

In our preliminary investigations, we observed DCC of 1% SE, 1% PE, and deionized water after providing 5% CO_2 for 10 min. This was the initial media in which experiments were carried out with the addition of BG11 medium and algal inoculum. In this study, we observed that dissolved CO_2 content was 1.6 times and 1.4 times higher in 1% SE and 1% PE, respectively compared with DI water. This experimental observation suggested that 1% SE and 1% PE were efficient in the physical absorption of CO_2 compared with deionized water.

It has been observed that the rise in CO_2 is responsible for the rise in carboxylation activity of ribulose 1,5 bisphosphate carboxylase/oxygenase (RuBisCo) and simultaneous suppression in oxygenation activity, resulting in increased photosynthesis and cell growth (34). It has also been seen that, under atmospheric CO_2 concentration, the activity of RuBisCo is even less than half of its catalytic capacity (35). Therefore, CO_2 enrichment in the case of 1% SE and 1% PE might have enhanced the RuBisCo activity which accelerated the microalgal cell growth.

241 The decrease in microalgal growth in control was probably because of the reduction in the
242 amount of CO_2 captured by the atmosphere compared with nanoemulsions. The higher carbon
243 dioxide content in nanoemulsions was supported by the pH measurement of nanoemulsions
244 substituted microalgal cultures. As shown in Figure.3, the change in pH observed in control
245 (~41%) was comparatively lower than the change in pH observed in 1% SE (~89%) and 1% PE
246 (~90%). The increase in pH was observed in cultivation with 1% PE (~ 5.4 to 10.3) and 1% SE
247 (~ 5.2 to 9.9) nanoemulsion, which was probably due to an increase in hydroxyl ion
248 concentrations during uptake of bicarbonates and CO_3^{-2}. In the case of 1% PE substituted algal
249 cultivation, the CO_3^{-2} could be the dominant species which probably increased the pH value
250 above 10. Since the pH change was higher, it suggests that more microalgal cells replicated
251 compared with control. It is because of the rise in pH corresponds to the algal growth (36). This
252 study suggested that the 1% SE and 1% PE act as suitable alkalescent culture media which was
253 appropriate for the growth of microalgae (37).
254 Furthermore, chlorophyll-a content of *C. pyrenoidosa* cultivated in two nanoemulsions and
255 control as a function of culture time was investigated. During chlorophyll analysis, it was found
256 that 1% SE and 1% PE enhanced chl-a pigment synthesis by 76% and 53% compared with
257 control (Figure. 2). The increase in chlorophyll concentrations in nanoemulsions could be due to
258 the sufficient availability of CO_2 to the microalgal cells.
259 In addition to this, a slight decrease (~15%) in chl-a content was observed in microalgal cells of
260 1% PE compared to 1% SE. This change is directly linked with the rise in pH during microalgal
261 cultivation. Increased pH results in the volatilization of ammonia (38). The volatilization of
262 ammonia affects the N metabolism of algal cells and creates nitrogen limiting conditions inside
263 algal cells. This impacts the chlorophyll content in microalgae (39). Literature also suggests that

the increase in CO_2 concentration leads to acidification of the algal cultivation system. This results in the replacement of Mg^{+2} with H^+ and the formation of pheophytin instead of chlorophyll (40). Salehi et al., 2019 studied the effect of n-alkane on *Chlorella vulgaris* and reported that the existence of hydrocarbons in the medium increases the permeability of the cell wall, resulting in the accumulation of hydrocarbons inside the algal cell (41). This might be the reason for inconsistency between chlorophyll concentration and cell concentration in case of 1% PE because n-alkanes are the major portion of paraffin oil.

Hence, overall it can be summarized that 1% SE and 1% PE nanoemulsions act as active CO_2 carriers which promote microalgal growth and chl-a synthesis comparative with conventional growth media (BG11).

At the end of 12 days, the *C. pyrenoidosa* biomass obtained in both the nanoemulsions was higher compared with control (~1.03 g L^{-1}) (Figure.4). Also, the biomass yield of *C. pyrenoidosa* was higher in 1% PE (~3.2 g L^{-1}) than 1% SE (~2.75 g L^{-1}). Table.2 highlights the biomass yield of *Chlorella* species obtained using different growth media by various researchers. Out of these, Wong, 2017 used five different media to grow *Chlorella* species and got maximum biomass productivity (1.42 gL^{-1}) using Bold Basal Media (42). In other such study, Prajapati et al., 2014 found the biomass productivity of (0.98 gL^{-1}) using Tap media (23). To efficiently deliver CO_2 to algal cells, Zheng et al. in 2016 used a membrane-based system and found an increase in biomass productivity (43). The maximum biomass yield achieved was 1.77gL^{-1} with CO_2 loading. Interestingly, the biomass yield in 1% SE and 1% PE was higher compared to all the reported studies so far, signifying the importance of this cultivation media.

The reason for this high productivity could be that the silicone and paraffin oil of nanoemulsions acts as an organic phase in which carbon dioxide is absorbed physically and diffuse into the

aqueous phase. A similar study was performed by Sawdon and Peng, 2014., using PFc emulsion for the cultivation of C. *vulgaris* in tubular photobioreactor and observed increased in microalgal cell concentration 4-folds, because of efficient CO_2 delivery to microalgal cells by PFc emulsion (44). Apart from this, silicone oil had also been studied in delivery of respiratory gases (CO_2 and O_2) in microbial cultivation (45), mammalian cell culturing (46) and in human retinal treatment (47).

Additionally, the cell counting was performed for observing the microalgal cell population in 1% SE, 1% PE and control (Figure. 5). Cell counting was performed on the 12^{th} day of the experiment using a cell counter. 1% PE had the maximum cell number ($3.0 \pm 0.21 \times 10^6$ cells ml^{-1}), followed by 1% SE ($2.4 \pm 0.30 \times 10^6$ cells ml^{-1}) and control ($1.34 \pm 0.09 \times 10^6$ cells ml^{-1}). The cell number was in agreement with the cell growth and biomass yield obtained from 1% PE and 1% SE nanoemulsions. Hence, from the present study, it was concluded that the 1% SE and 1% PE have successfully enhanced the potential of BG11 media by acting as an efficient CO_2 supplement for algal growth.

However, the dissolved CO_2 concentration of 1% SE was higher than the 1% PE but the microalgal growth, cell count and biomass yield obtained was higher in 1% PE supplemented microalgal cultivation. This is due to the chemical composition of paraffin oil and most probable explanations were highlighted in section 4.

3.4. MTT, SYTOX Staining:

The viability of cell indicates reproducibility of cells and also represent the physiological state which involves the production of enzymes like oxidoreductase, etc. (48). To determine algal and

cyanobacterial viability, tetrazolium compounds were introduced for viability assessment (49). Lately, studies suggested that MTT (3-[4,5-dimethylthiazol-2-yl]-2,5-diphenyl tetrazolium bromide) assay proved as a viable tool for viability assessment of algae and cyanobacteria. Therefore, the study aims with the viability testing of microalgal cells grown in 1% SE and 1% PE emulsion on the 8th day of cultivation by MTT assay. Based on the growth curve, the 8^{th} day was selected for MTT analysis as the microalgal culture started to move from the log phase to the stationary phase during this period. The sensitivity of the MTT assay is based on the ability of succinate dehydrogenase, microalgal mitochondrial enzyme, to convert MTT to a water-insoluble formazan dye in viable cells. The formation of formazan dye is directly correlated to cell viability and appears purple. The viability of cells is based on the intensity of purple color, which shows that darker the color, the more the viability in cells (Figure. 8) . In our case (Figure. 6), PE nanoemulsion gave the maximum cell viability (94%), followed by SE (77%) and control (53%). The results suggest that 1% PE and 1% SE nanoemulsions were non-toxic to the microalgal cells. Further, using SYTOX Green and fluorescence microscopy, a clear distinction between live and dead cells was observed. The observations confirmed that most of the microalgal cells cultivated in 1% SE and 1% PE had intact chloroplasts and membranes (Figure.7). Most of the cells emitted red autofluorescence and only few cells were stained by the green fluorescent dye SYTOX Green. On the other hand, control culture gave large patches of green emissions under a fluorescence microscope which confirmed the death stage of microalgal cells in BG11. Healthy or viable cells were highly efficient in reproducibility which indirectly increases cell density of microalgae. Therefore results suggest that microalgal cells cultivated in 1% PE are more viable followed by 1% SE compared with control which was cross-examined by

SYTOX, and obtained that live cells were higher in 1% PE and 1% SE compared with control (i e, Alg-1% PE>Alg-1% SE> Control).

3.5. Characterization

3.5.1. Bio-compositional analysis

The bio-compositional analysis was performed to evaluate the quantitative changes in macromolecules (protein, lipids, and carbohydrates) of harvested microalgal biomass cultivated in 1% SE and 1% PE compared to control (Table:2).

It has been studied that as the stationary stage of cell growth comes, nutrient depletion condition occurs which results in a shift of carbon to storage compounds like carbohydrates and lipids (35). An elevated CO_2 concentration in microalgal cells could trigger the Calvin cycle, resulting in the conversion of available CO_2 into biomolecule syntheses like carbohydrates and lipids. The pathways for biosynthesis of lipids and carbohydrates compete for the same carbon source, with carbohydrate synthesis requiring less energy than lipids (35). The carbohydrate content of microalgal biomass recovered from 1% SE and 1% PE was ~18.9% and 17.2% respectively, which was higher than control. Carbohydrates are the major synthetic products of carbon fixation metabolism. The finding suggests that an increase in the availability of CO_2 to microalgal cells in cultivation media is the influencing factor of carbohydrate synthesis inside microalgal cells (50). Additionally, an increase in lipid content in algal biomass obtained from 1% SE (23.6 % ± 0.848) and 1% PE (26.8%±0.848) with respect to control (18.05% ± 0.353). Interestingly, in both the nanoemulsions, the highest lipid content was observed in microalgal biomass harvested from 1% PE.

The protein content was slightly enhanced in 1% SE cultivated microalgal cells (53.75% ± 0.0707) compared to control, indicating they can be used as aquaculture feedstock, which desires protein content in the range of 35 to 60 wt% (51). The protein content of microalgal biomass harvested from 1% PE (~47%) decreased compared with microalgal biomass of control (~51%) and 1% SE (~53%). The high concentration of CO_2 affects the N metabolism of algal cells indirectly. As an outcome, the assimilation of nitrogen inside algal cells increases which create nitrogen limiting condition (52). Therefore, the concentration of protein, as well as chlorophyll decreases. This claim supports our experimental results obtained by 1% PE supplemented microalgal cultivation.

However, efficient lipid and carbohydrate content obtained from microalgal biomass recovered from nanoemulsions is a valuable property and may help in steady microalgal biomass generation without changing operating conditions. The results revealed that 1% SE and 1% PE supplemented media are efficient in enhancing the synthesis of carbohydrate, protein, and lipid.

3.5.2. FTIR Analysis

The microalgal samples were observed by using Fourier Transform Infrared (FTIR) technique (Table:3). From last decades FTIR spectroscopy has proven a powerful tool in the study of the biochemical composition of biological samples. The identification of peak is based on a comparison of the bands of the recorded FTIR spectra of algae with reference literature (22). The FTIR transmittance of the *C. pyrenoidosa* showed the presence of Si-O, P=O, C-OH, -CO, -COOH, functional groups (Figure. 9). IR spectra of *C. pyrenoidosa* showed higher intensity of lipid and carbohydrates functional groups from algal biomass of 1% SE and 1%PE. The strong peak at1652-1653 cm^{-1}, 1266 cm^{-1}, 1089 cm^{-1} representing amide I, protein, and nucleic acid

proteins were observed in microalgal biomass recovered from 1% SE. It supports the result obtained from biochemical characterization, suggesting biomass was rich in protein. The bands at 1200–950 cm^{-1} have shown absorption strength in biomass of both i.e., 1% SE and 1% PE which directs the presence of carbohydrate content compared to control. Two regions are commonly used for the assessment of lipid content. One is at 1740cm^{-1}, conveying stretching of the ester bond and other between 2800-3000cm^{-1} having methyl and methylene group. The strong absorption bands observed at 1456,1744, 2852, 2922, 2924 cm^{-1}clearly shows the presence of membrane lipids and lipids representing CH_2, CH_3, C=O groups in biomass obtained from 1% SE and 1% PE compared with control. It was clearly visible from the FTIR spectra of nanoemulsions recovered biomass of *C. pyrenoidosa* that distinct fingerprints of lipids, carbohydrates, and proteins exist in the biomass. FTIR spectroscopy appears as a viable analytical tool to evaluate the biofuel potential of algae.

3.5.3 Microscopic Analysis:

The 12^{th} day biomass of *C. pyrenoidosa* was subjected to FESEM analysis to investigate the morphological variation in the cell structure. Figure: 10 a-1, 10 a-2, and 10 a-3 show the FESEM images of *C. pyrenoidosa* grown in BG11, 1% SE, and 1% PE. From all the three figures, it was evident that the cells were spherical and packed together. The size of the microalgal cells in control was 6 ±2 µm which was similar to the cell size in 1% SE and 1% PE (Figure: 10 a-2 and 10 a-3). The microalgal cells in control possess a smooth cell surface, which indicated that cells were healthy. In the case of nanoemulsions, the cells grown kept their basic shape, but the edges of the cell wall were not similar to cells of control. Most of the cells in nanoemulsions were

found in aggregation. The results showed that the cells had outer covering in both 1% SE and 1% PE. It might be due to the release of recalcitrant Extracellular polymeric substance (EPS) in the case of nanoemulsion. The EPS is a sticky substance that algal cells release and is made of organic components. The presence of enhanced CO_2 in 1% SE and 1% PE nanoemulsions might have triggered the microalgal cells to release this substance. It has been reported that the elevated CO_2 concentration stimulates the metabolic carbon flux of algal cells and in order to maintain carbon balance, algae excrete organics like EPS (53). Also, figure 10 a-2 and 10 a-3 suggest that cells were morphologically intact with no cell damage, which indicates the good integrity of algal cells.

3.6. Other possible mechanisms for improved algal growth in nanoemulsions:

It should be noted that the nanoemulsions used in the proposed study possess higher solubility of CO_2 compared with conventional growth media. However, it was not obvious that the higher solubility of CO_2 was the only reason for increased microalgal growth in nanoemulsions substituted algal growth media. Based on literature several other factors could have resulted in greater microalgal biomass productivity in conjugation with nanoemulsions. Some of the possible mechanisms are summarized as follows:

- In our preliminary investigations, a higher concentration of oil (1%, 2%, 3%, 4%, and 5%) was used to observe the growth of *C. pyrenoidosa*. The high concentration of oil was supposed to enhance dissolved CO_2 concentration in nanoemulsion, but microalgal cell concentration declined at a higher concentration of oil like 3%, 4%, 5% (13). The results suggested that an increase in silicone oil concentration leads to a decrease in microalgal

415 growth. Hence, the inference was that diminished microalgal cell growth was probably
416 due to the scattering of light which reduces the depth penetration of light in the
417 microalgal culture. Therefore, lower concentration was used for the cultivation of
418 microalgae in the proposed study.

419 • Sawdon and Peng, 2014 has reported the use of perfluorocarbon (PFC) to improve algal
420 photosynthesis by decreasing dissolved oxygen in a tubular photobioreactor (44). The
421 mechanism proposed by the authors was the absorption of oxygen by the PFC suspended
422 in the culture which was produced by the algal cells during photosynthesis. In the
423 proposed study also, the organic compounds possess higher solubility of oxygen (54)
424 compared to water or the conventional growth media. Therefore, these organic solvents
425 (silicone and paraffin oil) might help to decrease oxygen content in the continuous phase
426 of nanoemulsions which indirectly promotes photosynthesis. However, more controlled
427 experiments need to be carried out to observe the impact of reduced oxygen in the algal
428 cultivation systems.

429 • Earlier studies have been reported that nanosuspension can also enhance the mass transfer
430 of solutes (55). In a quiescent fluid, diffusion is the main mechanism for mass transfer. For
431 the case of nanosuspensions, in addition to diffusion, due to the Brownian motion of the
432 suspended particles/droplets local disturbance velocity fields are also generated (56). The
433 resultant microscale convection of the fluid can enhance the mass transfer rates of solutes
434 in a suspension. In the present study also, the droplets of oil could be contributing to
435 improved mass transfer of nutrients, dissolved gases, etc. from the bulk growth media to
436 the algal cells.

- Scattering and absorption of light by the suspended particles in a suspension reduces the availability of light in a media and can lower the rate of photochemical reactions (57). However, the nature of suspended particles is transparent and used in a small volume, we observed that the residence time of light inside the suspension can increase (manuscript under preparation). Both the oils used in the proposed work were used in a small volume and transparent, which suggests that the increase in the residence time of light inside nanoemulsions. This might improve the light availability in the nanoemulsions supplemented media and the microalgal cells can efficiently utilize light to carry out photosynthesis.
- Paraffin components were found as a stimulant for algal growth at lower concentrations (58,59). In general, the lower carbon content oil phase can work as a source of carbon to the algal cells. This could be the possible reason for the phenomenal increase in microalgal growth in 1% PE along with enhanced CO_2 availability for microalgal growth.

4. Conclusions:

The present study proved that oil-in-water based colloidal system offers a possibility of increasing microalgae production and volumetric productivity in batch systems without compromising the microalgae cellular structure. A significant enhancement in pigment synthesis (chl-a) and biomass was observed. Also, the substantial increase in lipid content was obtained during nanoemulsion-based microalgal cultivation. The absorption of CO_2 in emulsions is the possible mechanism by which biomass productivity was increased. Moreover, the biomass productivity achieved in the present study is excellent using *Chlorella* species in different

458 nanoemulsions supplemented growth media. Therefore, 1% SE and 1% PE nanoemulsions are
459 projected as efficient support mediums that could significantly boost microalgal productivity.

460 This research gave us the option to explore various biocompatible oils for the mass cultivation of
461 algae. The next step would be to check the recyclability of the emulsion and testing it with actual
462 sources of CO_2 such as flue gas. The integration of the engineering approach with biotechnology
463 might help in making the algal cultivation process more feasible at a large scale in the future.

464 **Abbreviations:**

465 SE=1% Silicone oil nanoemulsion; PE= 1% Paraffin oil nanoemulsion; Alg-1% SE = Algal cells
466 in 1% Silicone oil nanoemulsion; Alg-1% PE = Algal cells in 1% Paraffin oil nanoemulsion; chl-
467 a = Chlorophyll-a; OD_{680} = Optical Density at 680nm, Deionized water =DI, Dissolved CO_2
468 concentration = DCC

469 **Acknowledgments:**

470 This research was financially supported by Indian Institute of Technology, Delhi. Dr. Arghya
471 Bhattacharya and Rahul Jain, CRDT, IIT Delhi are acknowledged for their assistance in the
472 preparation of manuscript.

473 **Authors' Contributions**

474 All authors contributed via scientific discussions during the work. H.N planned and performed
475 experiments, data analysis, and drafted the manuscript. A.M and V.S contributed to the design of

the experiments, coordination of experiments, and drafted the manuscript. All authors read and approved the final manuscript.

Funding

The proposed work was supported by Faculty Interdisciplinary Research Project (FIRP), IIT Delhi.

Availability of data and materials

The datasets during the current study available from the corresponding author on reasonable request.

Ethics approval and consent to participate

Not applicable.

Consent for publication

All authors approved the manuscript.

Competing interests

The authors declare that they have no competing interests

Author details

[1]Applied Microbiology Laboratory, Centre for Rural Development and Technology, Indian Institute of Technology Delhi, Hauz Khas, 110016, India.

[2] Department of Chemical Engineering, Indian Institute of Technology Delhi, Hauz Khas, New Delhi 110016, India.

REFERENCES:

1. Moreira D, Pires JCM. Atmospheric CO2 capture by algae: Negative carbon dioxide emission path. Bioresour Technol. 2016;215(2016):371–9.

2. Duarte JH, Fanka LS, Costa JAV. Utilization of simulated flue gas containing CO2, SO2, NO and ash for Chlorella fusca cultivation. Bioresour Technol. 2016;214(x):159–65.

3. Zheng Q, Martin GJO, Kentish SE. Energy efficient transfer of carbon dioxide from flue gases to microalgal systems. Energy Environ Sci. 2016;9(3):1074–82.

4. Duan Y, Guo X, Yang J, Zhang M, Li Y. Nutrients recycle and the growth of Scenedesmus obliquus in synthetic wastewater under different sodium carbonate concentrations. R Soc Open Sci. 2020;7(1).

5. Rosa GM, Morais MG, Costa JAV. Fed-batch cultivation with CO2 and monoethanolamine: Influence on Chlorella fusca LEB 111 cultivation, carbon biofixation and biomolecules production. Bioresour Technol. 2019;273(November 2018):627–33.

6. Zhang Z, Chen F, Rezakazemi M, Zhang W, Lu C, Chang H, et al. Modeling of a CO2-piperazine-membrane absorption system. Chem Eng Res Des. 2018;131:375–84.

7. Baena-Moreno FM, Rodríguez-Galán M, Vega F, Alonso-Fariñas B, Vilches Arenas LF, Navarrete B. Carbon capture and utilization technologies: a literature review and recent advances. Energy Sources, Part A Recover Util Environ Eff . 2019;41(12):1403–33.

8. Zheng Q, Martin GJO, Wu Y, Kentish SE. The use of monoethanolamine and potassium glycinate solvents for CO2 delivery to microalgae through a polymeric membrane system. Biochem Eng J. 2017;128:126–33.

9. Zheng Q, Xu X, Martin GJO, Kentish SE. Critical review of strategies for CO2 delivery to large-scale microalgae cultures. Chinese J Chem Eng. 2018;26(11):2219–28.

10. Shamiri A, Shafeeyan MS, Tee HC, Leo CY, Aroua MK, Aghamohammadi N. Absorption of CO2 into aqueous mixtures of glycerol and monoethanolamine. J Nat Gas Sci Eng. 2016;35:605–13.

11. Lawrence V. Dressler, Cranston, Alexander Chirkov, Lincoln. Method for producing algae in photobioreactor. US20090151241A1; 2008 Jun 12.

12. Akbas E, Soyler B, Oztop MH. Formation of capsaicin loaded nanoemulsions with high pressure homogenization and ultrasonication. Lwt. 2018;96(May):266–73.

13. Vikram Singh, Harshita Nigam, Anushree Malik. “Method for sequestering carbon-di-oxide by enhancing algal growth, and applications thereoff.” India; 2018.

14. Jeong M, Lee JW, Lee SJ, Kang YT. Mass transfer performance enhancement by nanoemulsion absorbents during CO2absorption process. Int J Heat Mass Transf . 2017;108:680–90.

15. Anshu Bala Yakub. Study of waste water quality of milk processing unit. Study waste water Qual milk Process unit its Util. 2010;17–42.

16. Brunale P, Santana H, Cereijo CR, Nascimento RC, Sabaini PS, Brasil BSAF, et al. Microalgae cultivation in sugarcane vinasse: Selection, growth and biochemical

characterization. Vol. 228, Bioresource Technology. 2016. p. 133–40.

17. Chinnasamy S, Bhatnagar A, Hunt RW, Das KC. Microalgae cultivation in a wastewater dominated by carpet mill effluents for biofuel applications. Bioresour Technol. 2010;101(9):3097–105.

18. Porra RJ, Thompson WA, Kriedemann PE. Determination of accurate extinction coefficients and simultaneous equations for assaying chlorophylls a and b extracted with four different solvents: verification of the concentration of chlorophyll standards by atomic absorption spectroscopy. Biochim Biophys Acta - Bioenerg. 1989 Aug 1 ;975(3):384–94.

19. Jena U, Vaidyanathan N, Chinnasamy S, Das KC. Evaluation of microalgae cultivation using recovered aqueous co-product from thermochemical liquefaction of algal biomass. Bioresour Technol. 2011;102(3):3380–7.

20. Arumugam M, Agarwal A, Arya MC, Ahmed Z. Influence of nitrogen sources on biomass productivity of microalgae Scenedesmus bijugatus. Bioresour Technol. 2013;131:246–9.

21. Dubois M, Gilles KA, Hamilton JK, Rebers PA, Smith F. Colorimetric Method for Determination of Sugars and Related Substances. Anal Chem. 1956;28(3):350–6.

22. Fryer HJL, Davis GE, Manthorpe M, Varon S. Lowry protein assay using an automatic microtiter plate spectrophotometer. Anal Biochem. 1986;153(2):262–6.

23. Prajapati SK, Malik A, Vijay VK. Comparative evaluation of biomass production and bioenergy generation potential of Chlorella spp. through anaerobic digestion. Appl Energy. 2014;114:790–7.

555 24. Omar HH, Al-Judaibiand A, El-Gendy A. Antimicrobial, antioxidant, anticancer activity
556 and phytochemical analysis of the red alga, laurencia papillosa. Int J Pharmacol.
557 2018;14(4):572–83.

558 25. Eckersley E, Berger BW. An engineered polysaccharide lyase to combat harmful algal
559 blooms. Biochem Eng J. 2018;132:225–32.

560 26. Meng Y, Yao C, Xue S, Yang H. Application of fourier transform infrared (FT-IR)
561 spectroscopy in determination of microalgal compositions. Bioresour Technol.
562 2014;151:347–54.

563 27. Dananjaya SHS, Godahewa GI, Jayasooriya RGPT, Lee J, De Zoysa M. Antimicrobial
564 effects of chitosan silver nano composites (CAgNCs) on fish pathogenic Aliivibrio
565 (Vibrio) salmonicida. Aquaculture. 2016;450:422–30.

566 28. Hu YT, Ting Y, Hu JY, Hsieh SC. Techniques and methods to study functional
567 characteristics of emulsion systems. J Food Drug Anal. 2017;25(1):16–26.

568 29. Choi W, Kim G, Lee K. Influence of the CO 2 absorbent monoethanolamine on growth
569 and carbon fixation by the green alga Scenedesmus sp. Bioresour Technol. 2012;120:295–
570 9.

571 30. Wolfbeis OS, Kovács B, Goswami K, Klainer SM. Fiber-Optic Fluorescence Carbon
572 Dioxide Sensor for Environmental Monitoring. Mikrochim Acta. 1998;129(3--4):181–8.

573 31. Gonçalves AL, Rodrigues CM, Pires JCM, Simões M. The effect of increasing CO2
574 concentrations on its capture, biomass production and wastewater bioremediation by
575 microalgae and cyanobacteria. Algal Res. 2016;14:127–36.

32. Araújo SDC, Garcia VMT. Growth and biochemical composition of the diatom Chaetoceros cf. wighamii brightwell under different temperature, salinity and carbon dioxide levels. I. Protein, carbohydrates and lipids. Aquaculture. 2005;246(1–4):405–12.

33. Fábregas J, Otero A, Domínguez A, Patiño M. Growth rate of the microalga Tetraselmis suecica changes the biochemical composition of Artemia species. Mar Biotechnol. 2001;3(3):256–63.

34. Ghosh A, Kiran B. Carbon Concentration in Algae: Reducing CO2 From Exhaust Gas. Trends Biotechnol. 2017;35(9):806–8.

35. Varshney P, Beardall J, Bhattacharya S, Wangikar PP. Isolation and biochemical characterisation of two thermophilic green algal species- Asterarcys quadricellulare and Chlorella sorokiniana , which are tolerant to high levels of carbon dioxide and nitric oxide. Algal Res. 2018;30(December 2017):28–37.

36. Gerardi MH, Lytle B. The Biology and Troubleshooting of Facultative Lagoons. Biol Troubl Fac Lagoons. 2015;1–226.

37. Price GD. Inorganic carbon transporters of the cyanobacterial CO2 concentrating mechanism. Photosynth Res. 2011;109(1–3):47–57.

38. Kesaano M, Gardner RD, Moll K, Lauchnor E, Gerlach R, Peyton BM, et al. Dissolved inorganic carbon enhanced growth, nutrient uptake, and lipid accumulation in wastewater grown microalgal biofilms. Bioresour Technol. 2015;180:7–15.

39. Zhu S, Huang W, Xu J, Wang Z, Xu J, Yuan Z. Metabolic changes of starch and lipid triggered by nitrogen starvation in the microalga Chlorella zofingiensis. Bioresour

Technol. 2014;152:292–8.

40. Devi MP, Mohan SV. Bioresource Technology CO 2 supplementation to domestic wastewater enhances microalgae lipid accumulation under mixotrophic microenvironment : Effect of sparging period and interval. Bioresour Technol. 2012;112:116–23.

41. Salehi M, Biria D, Shariati M, Farhadian M. Treatment of normal hydrocarbons contaminated water by combined microalgae – Photocatalytic nanoparticles system. J Environ Manage. 2019;243(November 2018):116–26.

42. Wong Y. Growth Medium Screening for Chlorella vulgaris Growth and Lipid Production. J Aquac Mar Biol. 2017;6(1):1–10.

43. Zhang W, Bhubalan K, Decho AW, Dittrich M, Zhu T. Carbonate Precipitation through Microbial Activities in Natural Environment, and Their Potential in Biotechnology: A Review. 2016 ;4.

44. Sawdon A, Peng C. Internal deoxygenation of tubular photobioreactor for mass production of microalgae by perfluorocarbon emulsions. J Chem Technol Biotechnol 2014;(April).

45. Ramsey WS, Tanenholtz PEE. Means for Stimulating Microbial Growth, US Patent 4,166,006. 1979;(19):3–8.

46. Schulz C, Vogel JH, Scharfenberg K. Influence of Pluronic F-68 on the Ultrafiltration of Cell Culture Supernatants. Anim Cell Technol. 1997;373–8.

47. Inoue M, Iriyama A, Kadonosono K, Tamaki Y, Yanagi Y. Effects of perfluorocarbon

liquids and silicone oil on human retinal pigment epithelial cells and retinal ganglion cells. Retina. 2009;29(5):677–81.

48. Li J, Song L. Applicability of the MTT assay for measuring viability of cyanobacteria and algae, specifically for Microcystis aeruginosa (Chroococcales, Cyanobacteria). Phycologia. 2007;46(5):593–9.

49. Markelova AG, Vladimirova MG, Kuptsova ES. A comparison of cytochemical methods for the rapid evaluation of microalgal viability. Russ J Plant Physiol. 2000;47(6):815–9.

50. Ji MK, Yun HS, Hwang JH, Salama ES, Jeon BH, Choi J. Effect of flue gas CO2 on the growth, carbohydrate and fatty acid composition of a green microalga Scenedesmus obliquus for biofuel production. Environ Technol (United Kingdom). 2017;38(16):2085–92.

51. Jones SW, Karpol A, Friedman S, Maru BT, Tracy BP. Recent advances in single cell protein use as a feed ingredient in aquaculture. Curr Opin Biotechnol. 2020;61:189–97.

52. Singh SK, Rahman A, Dixit K, Nath A, Sundaram S. Evaluation of promising algal strains for sustainable exploitation coupled with CO2 fixation. Environ Technol (United Kingdom). 2016;37(5):613–22.

53. Li W, Xu X, Fujibayashi M, Niu Q, Tanaka N, Nishimura O. Response of microalgae to elevated CO2 and temperature: impact of climate change on freshwater ecosystems. Environ Sci Pollut Res. 2016;23(19):19847–60.

54. Chavan A, Madhusudan. Oxygen Mass Transfer in Biological Treatment System in the Presence of Non-aqueous Phase Liquid. APCBEE Procedia. 2014;9(1969):54–8.

639 55. Krishnamurthy S, Bhattacharya P, Phelan PE, Prasher RS. Enhanced mass transport in
640 nanofluids. Nano Lett. 2006;6(3):419–23.

641 56. Veilleux J, Coulombe S. A dispersion model of enhanced mass diffusion in nanofluids.
642 Chem Eng Sci. 2011;66(11):2377–84.

643 57. Alfano OM, Cabrera MI, Cassano AE. Modeling of light scattering in photochemical
644 reactors. Chem Eng Sci. 1994;49(24):5327–46.

645 58. Jiang Z, Huang Y, Xu X, Liao Y, Shou L, Liu J, et al. Advance in the toxic effects of
646 petroleum water accommodated fraction on marine plankton. Acta Ecol Sin.
647 2010;30(1):8–15.

648 59. Sciences L. Effects of Petroleum Oils and Their Paraffinic , Asphaltic , and Aromatic
649 Fractions on Photosynthesis and Respiration of Microalgae. 1990;16:8–16.

650 60. Khalili A, Najafpour GD, Amini G, Samkhaniyani F. Influence of nutrients and LED light
651 intensities on biomass production of microalgae Chlorella vulgaris. Biotechnol Bioprocess
652 Eng. 2015;20(2):284–90.

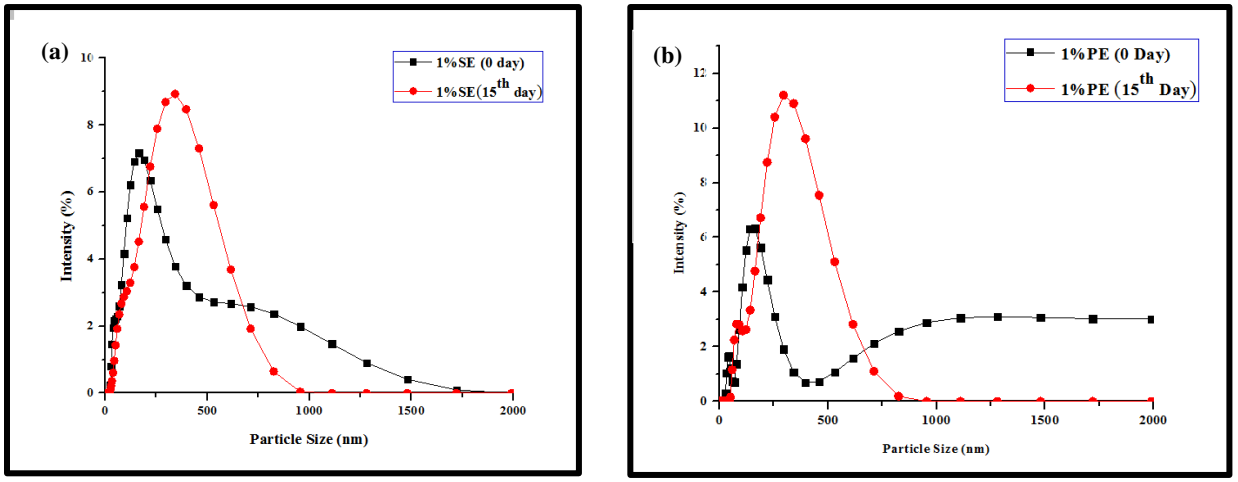

Figure 1: (a) DLS study of oil droplet size of 1% Silicone Oil Nanoemulsion 0^{th} day and 15^{th} day **(b)** DLS study of oil droplet size of 1% Paraffin oil nanoemulsion at 0^{th} day and 15^{th} day

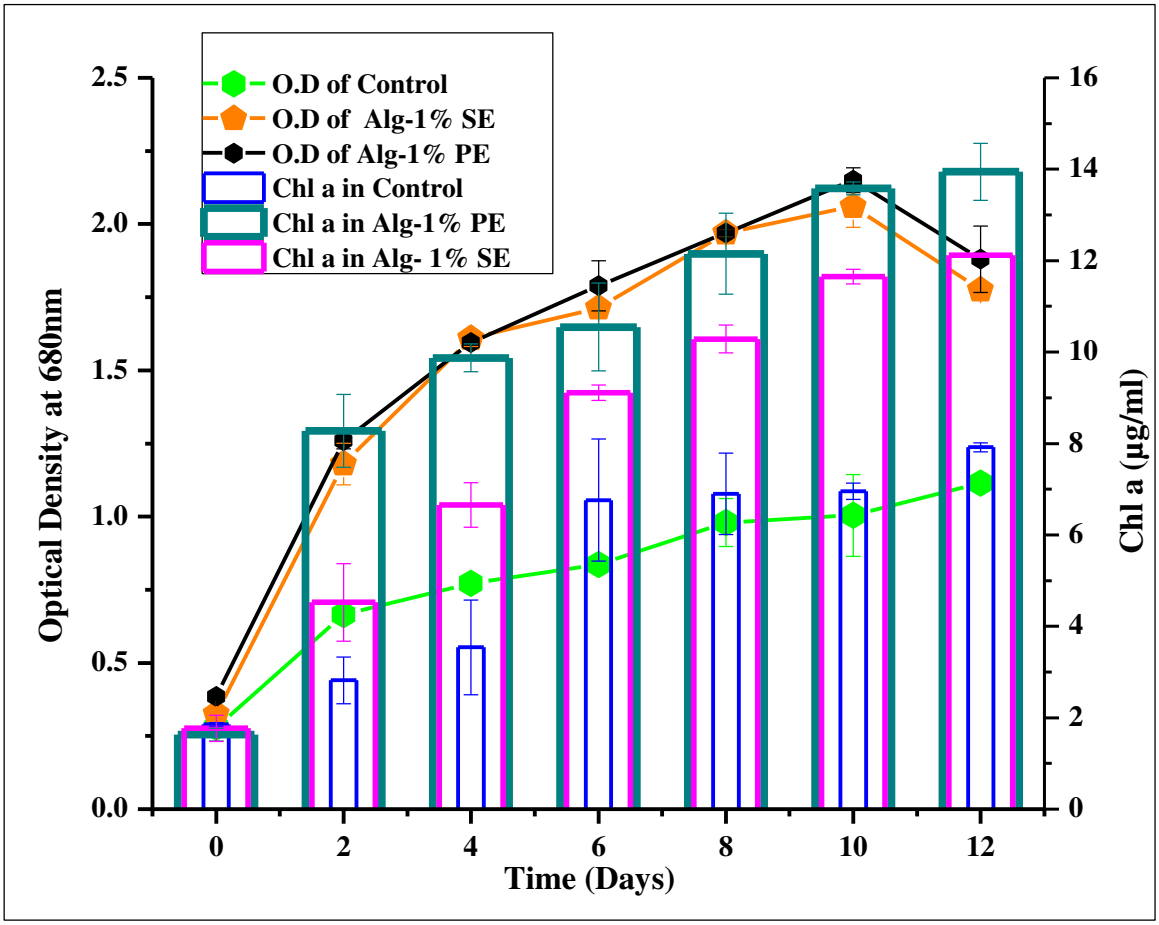

Figure 2: Growth profile of *C. pyrenoidosa* cultivated in 1% SE and 1% PE compared with control (BG11) in terms of OD_{680} and Chl- a content. Errors bars are shown ± SD.

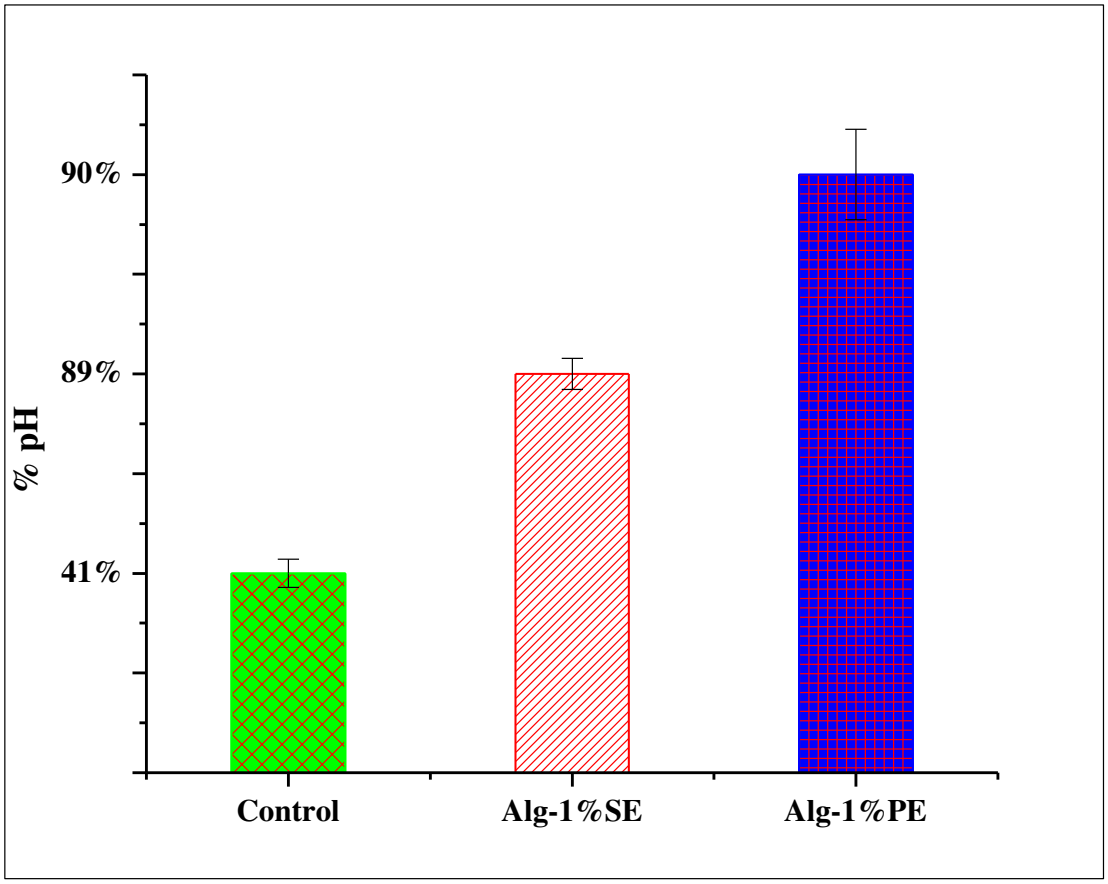

Figure 3: % pH change observed during cultivation of *C. pyrenoidosa* in 1% SE and 1% PE compared with control (BG11). Errors bars are shown ± SD.

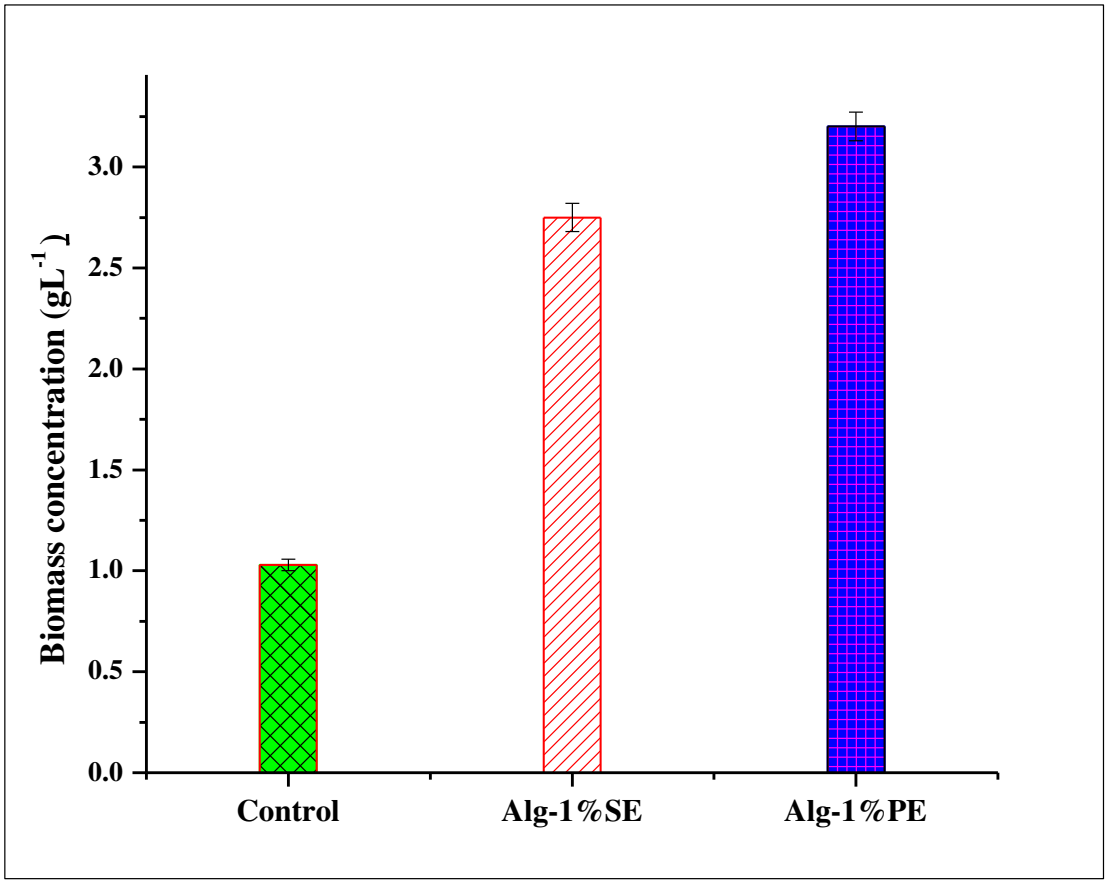

Figure 4: Comparison of biomass concentration of *C. pyrenoidosa* in 1%SE and 1%PE compared with control (BG11). Errors bars indicated are shown ± SD.

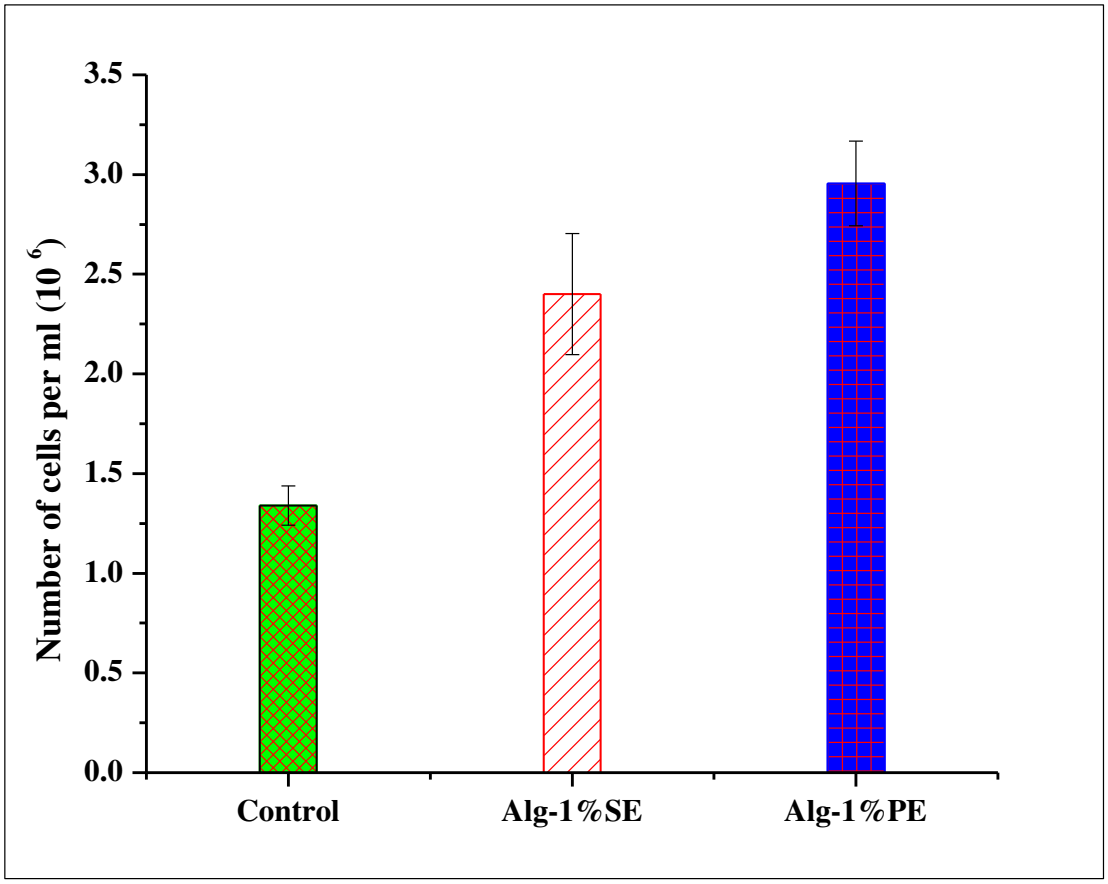

Figure 5: Cell count of *C. pyrenoidosa* cultivated in 1% SE, 1% PE and BG11(Control) on 12th day. Errors bars are shown ± SD.

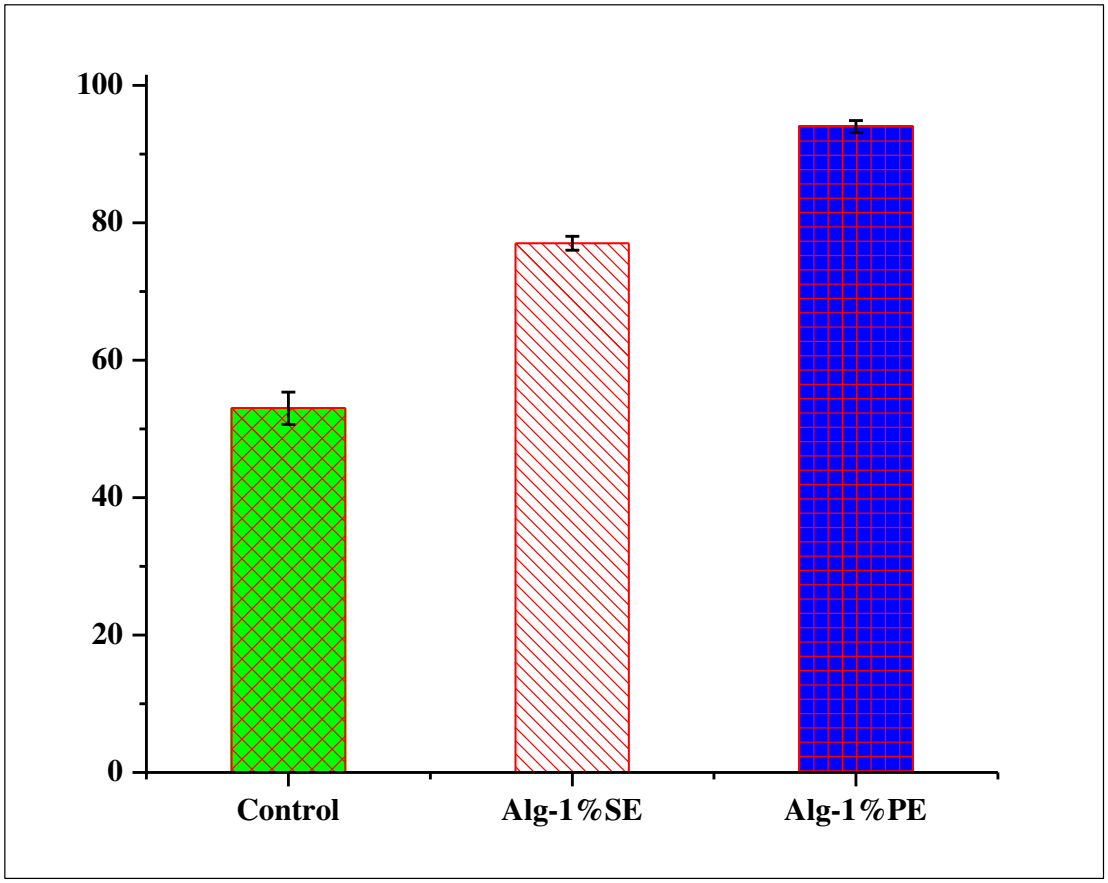

Figure 6: % Cell viability observation of *C. pyrenoidosa* performed by MTT Assay in 1% SE and 1% P E. Errors bars are shown ± SD in MTT analysis.

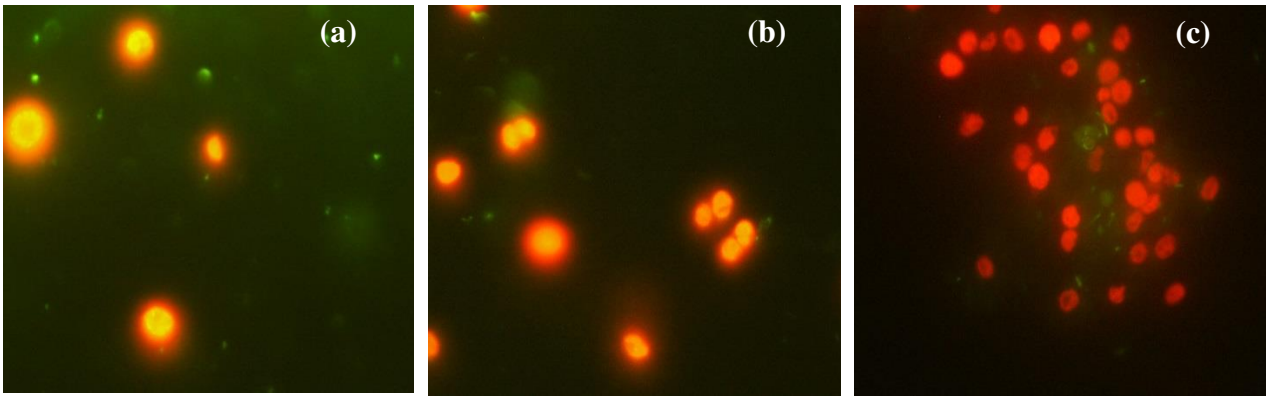

Figure 7: Live/dead discrimination of *C. pyrenoidosa* on 8 th day in **(a)** control. **(b)** 1% SE. **(c)** 1% PE. Live /dead discrimination of *C. pyrenoidosa* by SYTOX® Green staining. Live cells appear red (autofluorescence) while dead cells (SYTOX® Green stained) appear green or yellow color (scale bar: 100 μm).

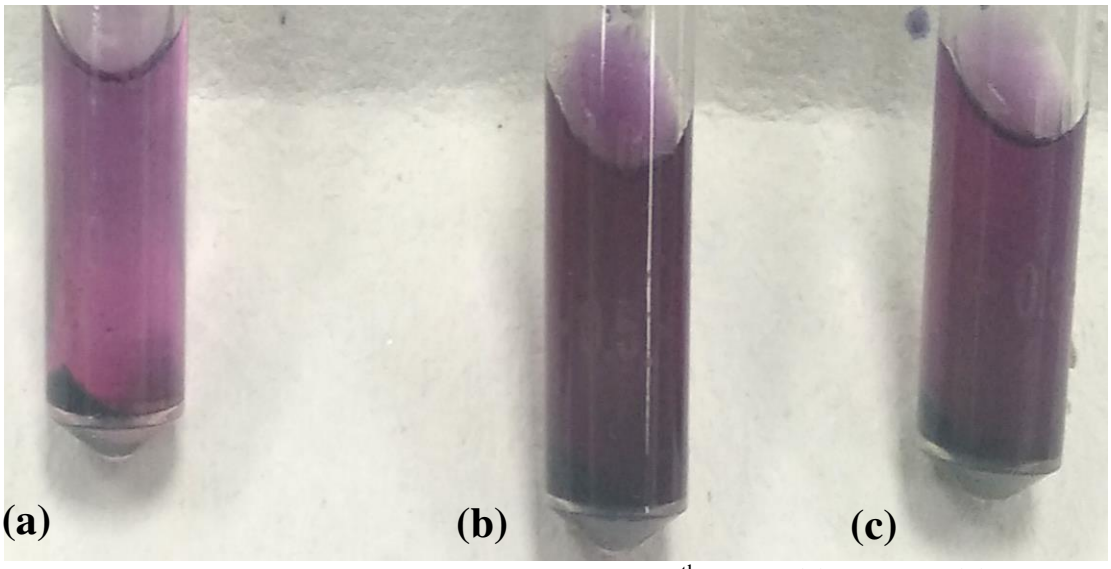

Figure 8: MTT cell viability assay of *C. pyrenoidosa* on 8th day in **(a)** Control. **(b)** 1% PE. **(c)** 1% SE

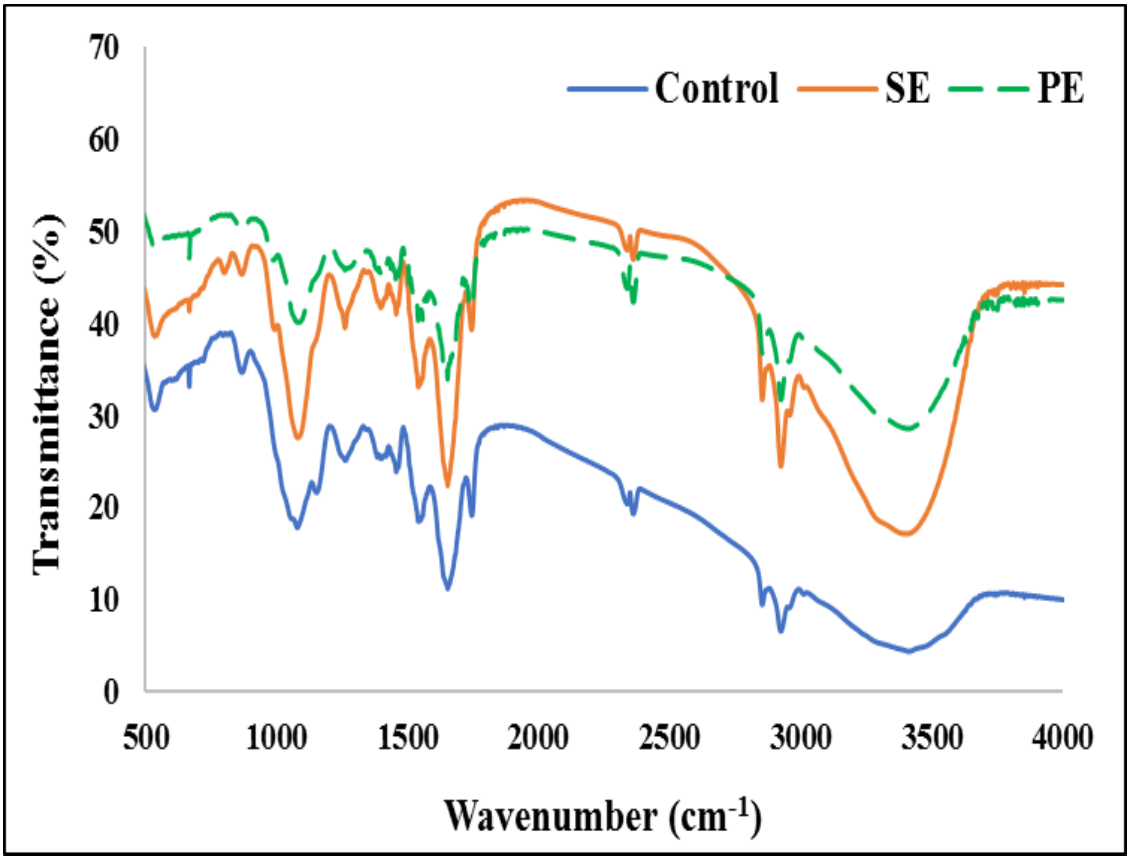

Figure 9: FTIR spectra of *C. pyrenoidosa* biomass cultivated in BG 11 (control), 1% SE and 1% PE.

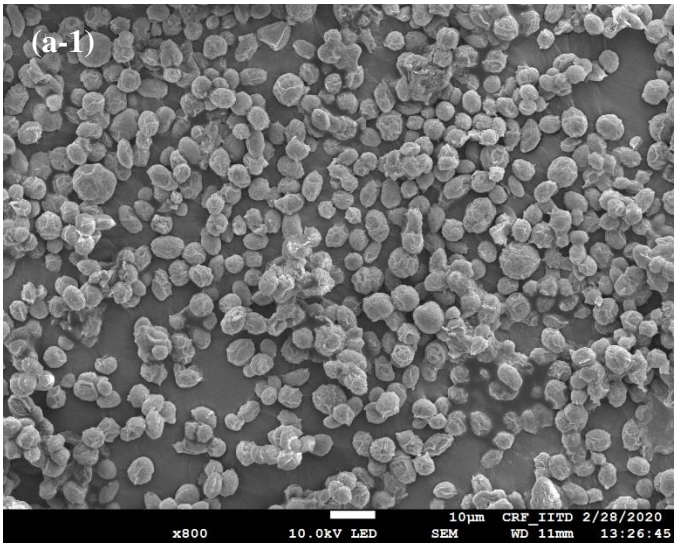
(a-1)
10µm CRF_IITD 2/28/2020
x800 10.0kV LED SEM WD 11mm 13:26:45

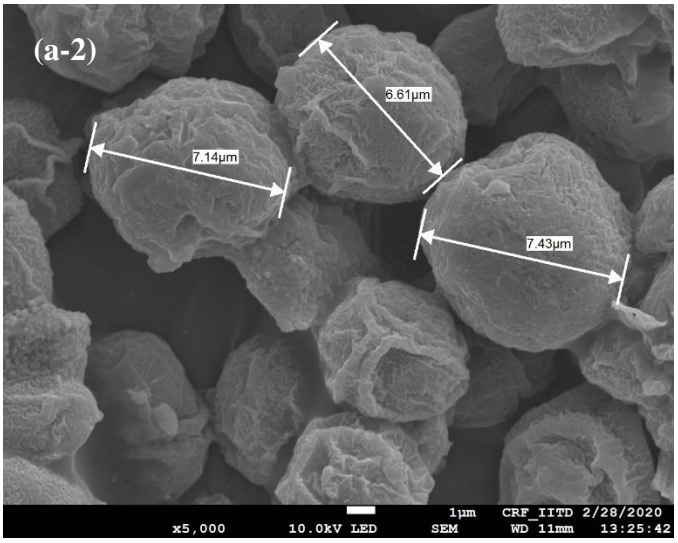
(a-2)
6.61µm
7.14µm
7.43µm
1µm CRF_IITD 2/28/2020
x5,000 10.0kV LED SEM WD 11mm 13:25:42

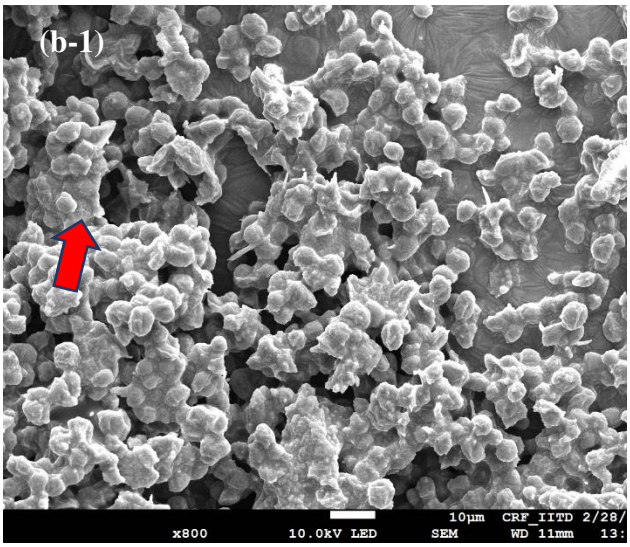
(b-1)
10µm CRF_IITD 2/28/
x800 10.0kV LED SEM WD 11mm 13:

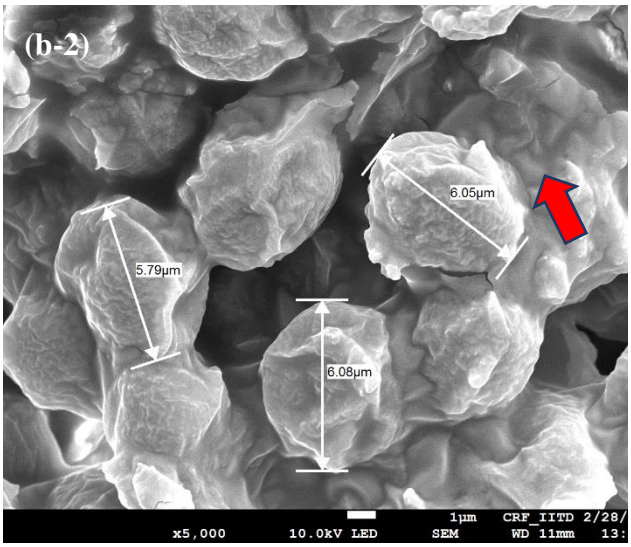
(b-2)
6.05µm
5.79µm
6.08µm
1µm CRF_IITD 2/28/
x5,000 10.0kV LED SEM WD 11mm 13:

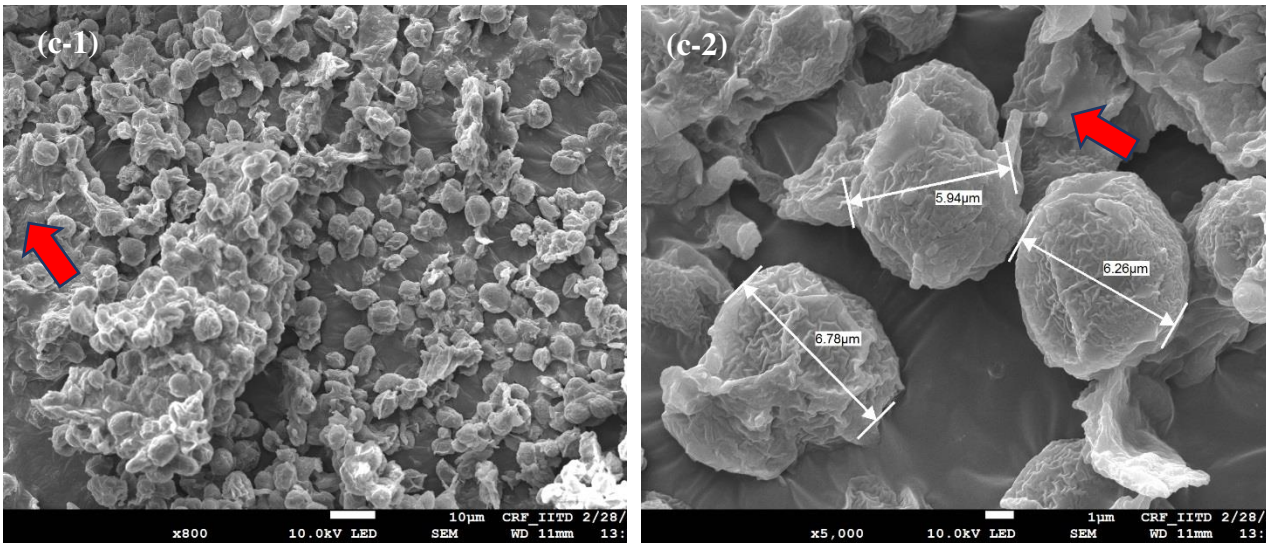

Figure 10. Field-emission scanning electron microscopy (FESEM) images of C. *pyrenoidosa*. (**a-1**) The image of cluster of cells of *C. pyrenoidosa* cultivated in BG11 i.e, control at 800x magnification; (**a-2**) The image of single cells of *C. pyrenoidosa* cultivated in BG11 i.e, control at 5000x magnification;((**b-1**)The image of cluster of cells of *C. pyrenoidosa* grown in 1% Silicon oil emulsion (SE) at 800x magnification; (**b-2**)The image of single cells of *C. pyrenoidosa* grown in 1% Silicon oil emulsion (SE) at 5000x magnification; (**c-1**) The image of cluster of cells of *C. pyrenoidosa* grown in 1% Paraffin oil emulsion (PE) at 800x magnification;**(c-2)** The image of single cells of *C. pyrenoidosa* grown in 1% Paraffin oil emulsion (PE) at 5000x magnification.

Table 1: Comparison of biomass yield of Chlorella *sp*.in different cultivation media

Growth Medium	Biomass yield (gL^{-1})	References
Bold Basal, Modified BG-11	1. 42 ± 0.012, 0.9±0.01	(42)
Carbonate Based Media at 0.5 and 0.7 loading concentration	1.63 ±0.10 and 1.77 ± 0.02	(3)
Urea +K_2HPO_4 + $MgSO_4 \cdot 7H_2O$ and Ammonium ferric citrate	1.37 g/L	(60)
Tap-water	0.98 ± 0.11	(23)
1% SE and PE amended with BG-11	2.75 ± 0.07 gL^{-1} and 3.2± 0.07gL^{-1}	Proposed study

Table 2: Biomass (biochemical) composition of *C. pyrenoidosa* (represented as mean ± SD).

Biochemical composition	Control	SE	PE
Carbohydrates	13.6 ± 0.565	18.9±0.282	17.2 ±0.565
Proteins	51.75±0.777	53.75 ± 0.0707	47.1±0.141
Lipids	18.05 ± 0.353	23.6±0.848	26.8±0.848

Table 3: Monitoring macromolecular changes in *C. pyrenoidosa* by FTIR analysis

Wavenumber range (cm^{-1})	**Assignments**	**Functional groups**	**Peak (cm^{-1})**
1064-880	-------	Carbohydrate	965
1090-1030	P=O or Si-O	Nucleic acids	1089
1150-1000	C-O/v Si-O	Polysaccharides/Siloxane (Carbohydrate peak/siloxane shoulder at 1200 cm^{-1})	1072
1263	C-O	Ester	1260
1275	C-O-H	Carbohydrates, proteins, DNA, and RNA	1266
1398-1370	CH_3, CH_2, C-O	Proteins, Carboxylic Groups	1394
1456-1450	CH_2, CH_3	Lipid, Protein	1456
1550-1640	N-H bending	Amide	1558
1655-1638	C=O	Protein (Amide I)	1652-1653
1745-1734	C=O of esters	Membrane Lipids, Fatty acids	1744
2875-2850	CH_2, CH3	Lipids	2852
2930-2920	CH_2	Lipids	2922,2924

Figures

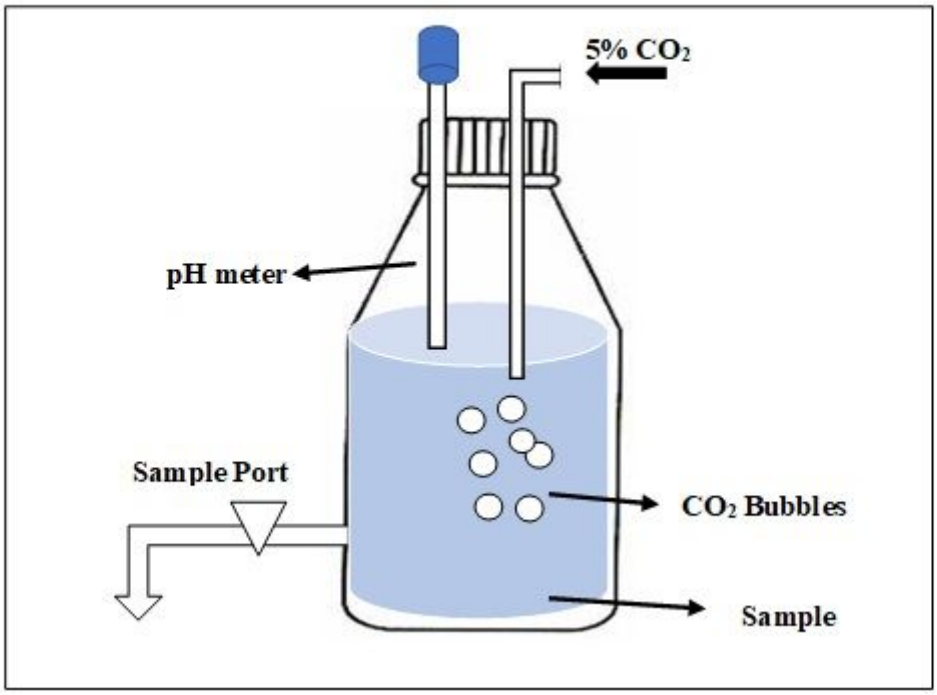

Figure 1

A schematic representation of dissolved free CO2 analysis

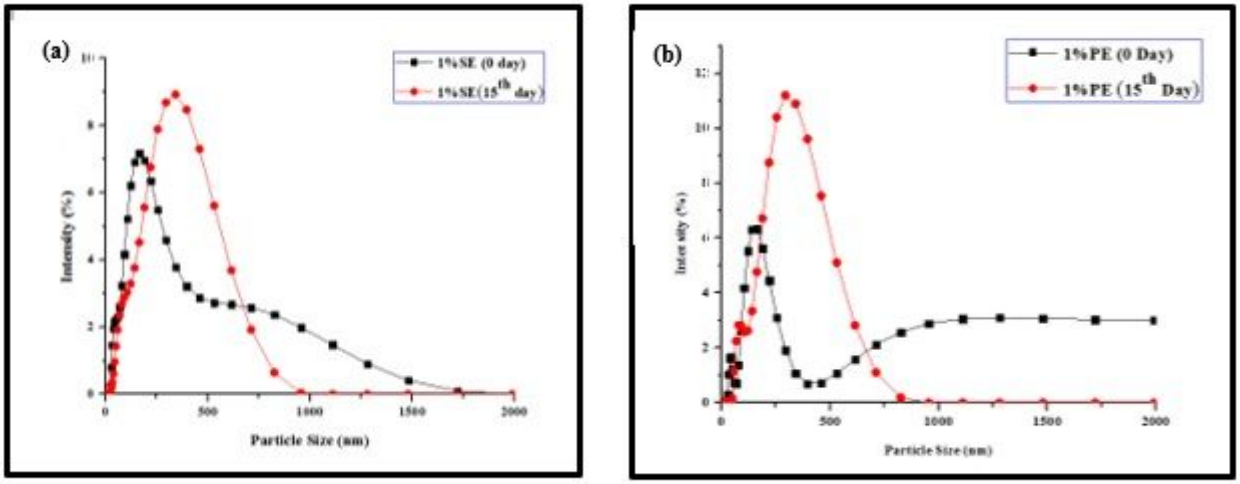

Figure 2

Comparison of droplet size distribution obtained from DLS for (a) 1% Silicone oil nanoemulsion (1% SE) on 0th day and 15th day (b) 1% Paraffin oil nanoemulsion (1% PE) on 0th day and 15th day

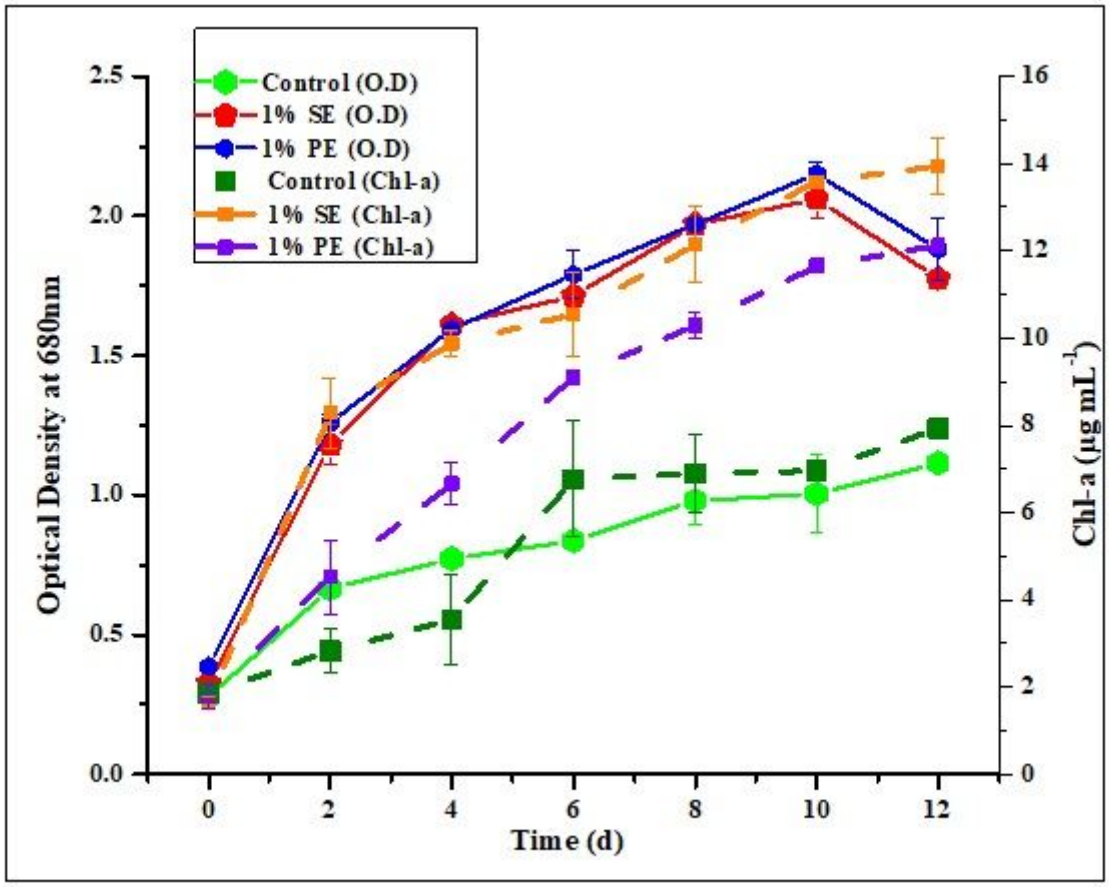

Figure 3

Growth profile and pigment synthesis of C. pyrenoidosa cultivated in 1% Silicone oil nanoemulsion (1% SE) and 1% Paraffin oil nanoemulsion (1% PE) compared with control (BG11) in terms of OD680 and Chl-a content. Solid lines in the figure represent optical density and broken lines display Chl- a synthesis. The microalgal growth and pigment synthesis were measured every 48 hours up to 12 days. The cultures were operated at 25 ± 1 °C with ~ 46.5 to 50 µmol m−2 s−1 light intensity for 12 days. The data shown are the average of two data points, and error bars represent standard deviation. Data followed by an asterisk (*) are significantly different from control ($p < 0.005$, analyzed by t-test).

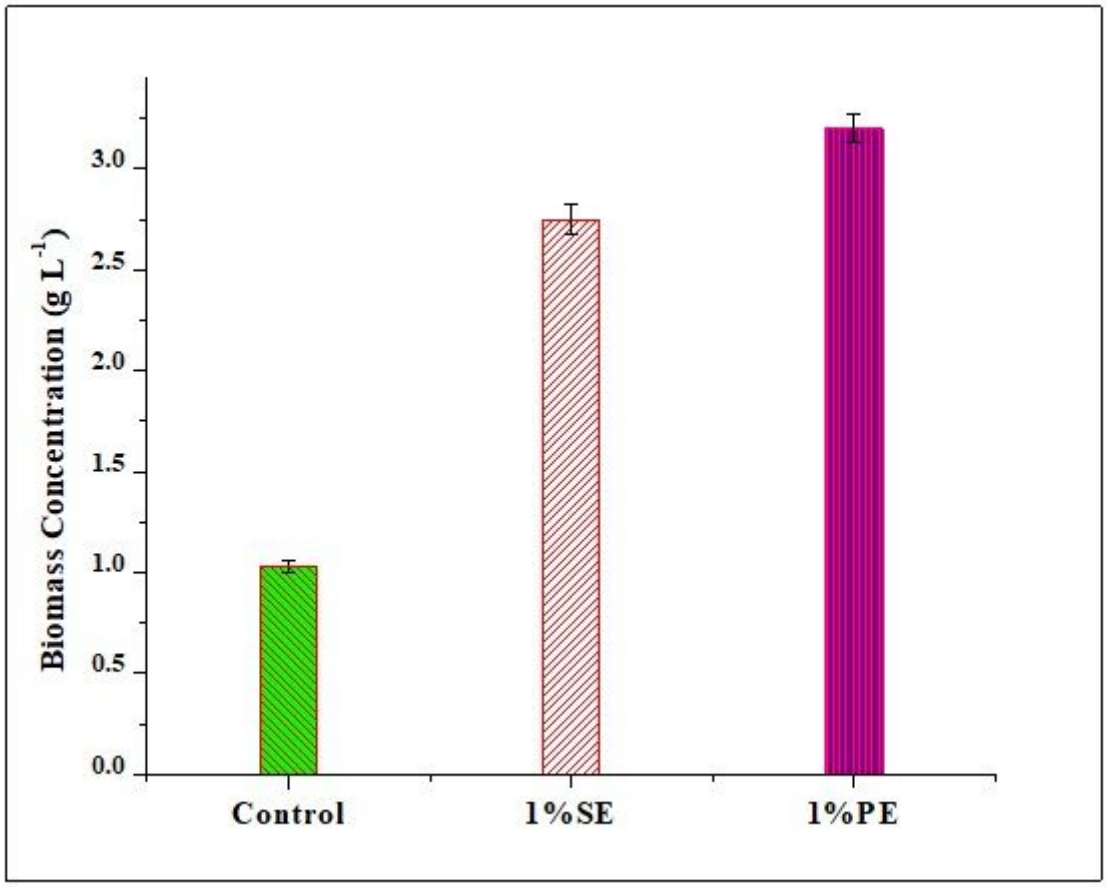

Figure 4

Growth profile of C. pyrenoidosa was observed in terms of biomass yield (g L-1) in 1% Silicone oil nanoemulsion (1% SE), 1% Paraffin oil nanoemulsion (1% PE), and control (BG11). The cultures were operated at 25 ± 1 °C with ~ 46.5 to 50 µmol m−2 s−1 light intensity for 12 days. The data shown are the average of two data points, and error bars represent standard deviation. Data followed by an asterisk (*) are significantly different from control ($p < 0.005$, analyzed by t-test).

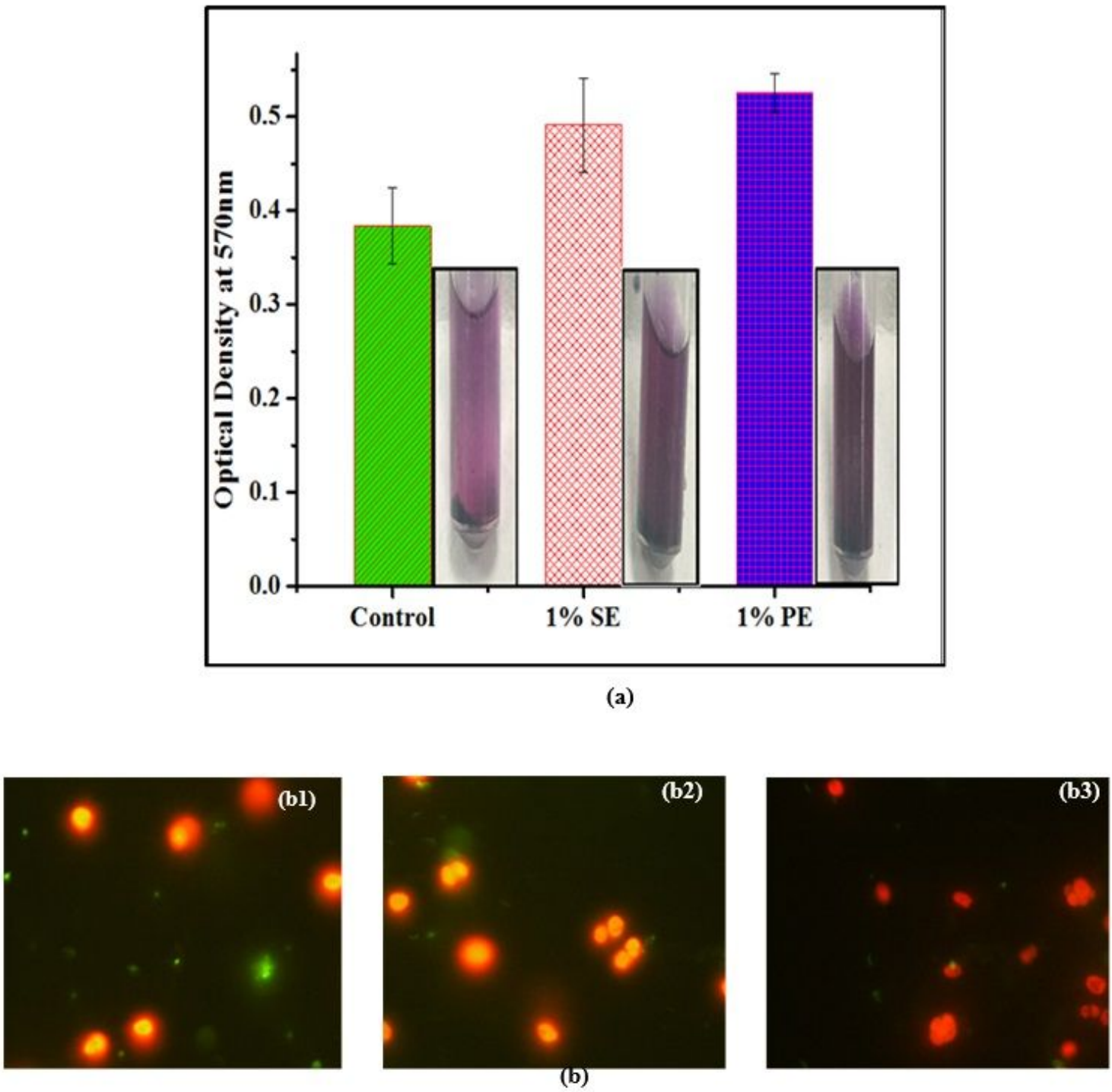

Figure 5

Microalgal cell viability analysis using MTT assay and SYTOX ® Green method (a) MTT result comparison of control (BG 11), 1% Silicone oil nanoemulsion (1% SE) and 1% Paraffin oil nanoemulsion (1% PE) in terms of optical density at 570 nm with corresponding vials showing purple formazan during the MTT Assay. Dark purple color represents greater cell viability. Errors bars are shown ± SD in MTT analysis. (b) SYTOX ® Green stained fluorescent micrographs of C. pyrenoidosa to differentiate live and

dead cells (b1) control (BG 11) (b2) 1% Silicone oil nanoemulsion (b3) 1% Paraffin oil nanoemulsion. Live cells appear red while dead cells appear green in color.

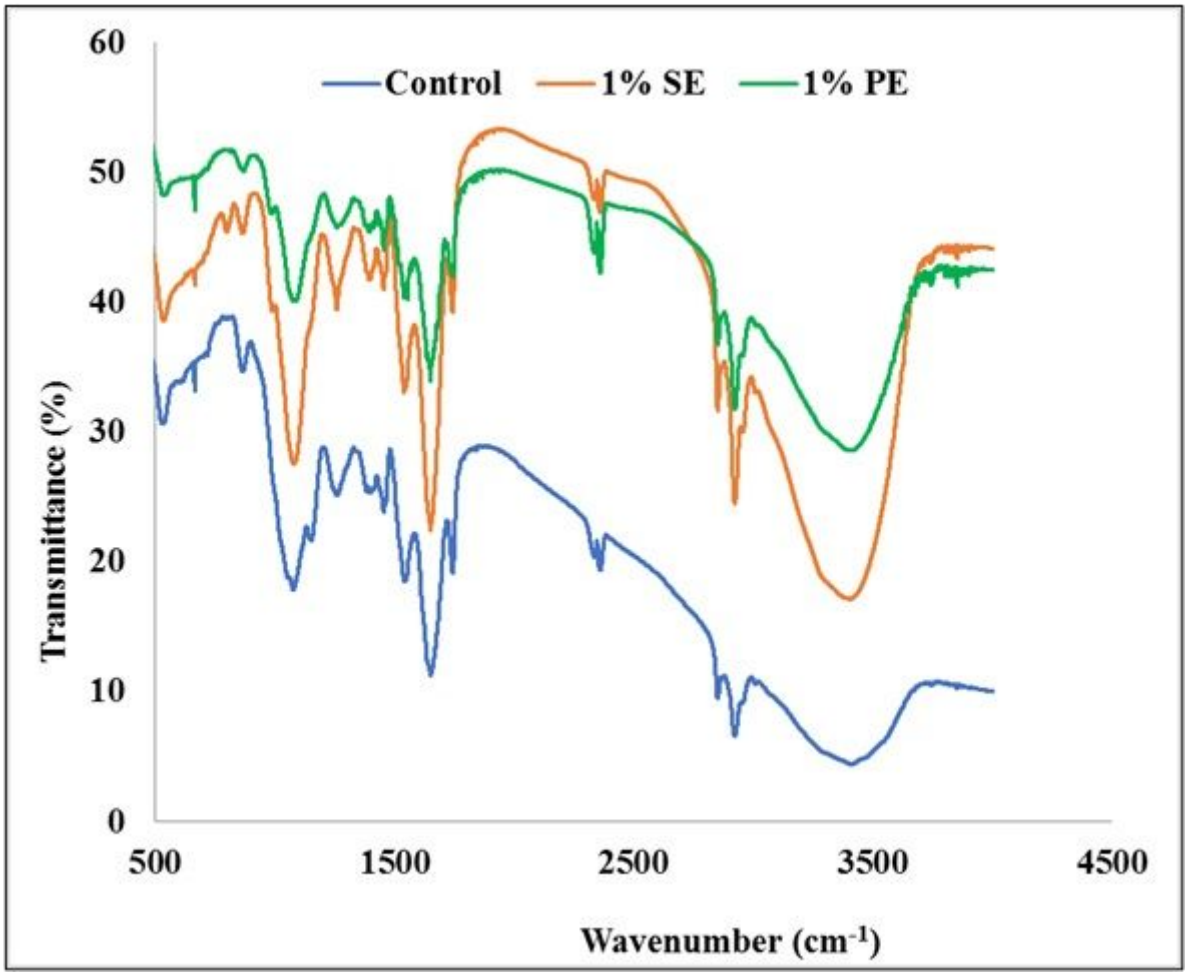

Figure 6

FTIR spectra of C. pyrenoidosa biomass obtained from control (BG 11), 1% Silicone oil nanoemulsion (1% SE), and 1% Paraffin oil nanoemulsion (1% PE) with different functional groups.

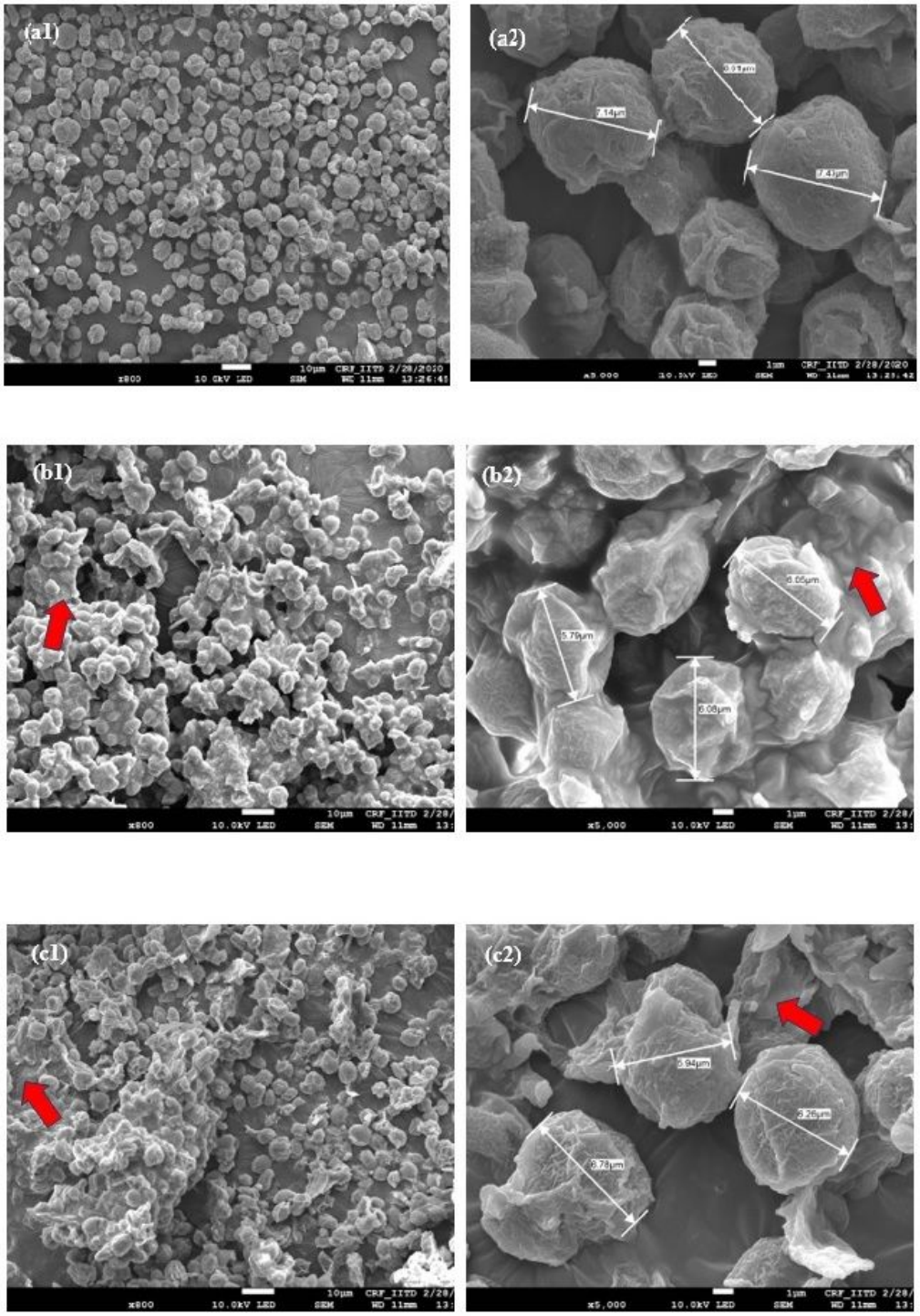

Figure 7

Field-emission scanning electron microscopy images of C. pyrenoidosa. Micrographs of BG 11 (control) cultivated C. pyrenoidosa at (a1) 800x magnification; (a2) 5000x magnification. Micrographs of 1% Silicone oil nanoemulsion (1% SE) cultivated C. pyrenoidosa at (b1) 800x magnification; (b2) 5000x magnification. Micrographs of 1% Paraffin oil nanoemulsion (1% PE) cultivated C. pyrenoidosa at (c1) 800x magnification; (c2) 5000x magnification.

Supplementary Files

This is a list of supplementary files associated with this preprint. Click to download.

- GraphicalAbstract.png
- Supplementary.pdf